Surfactant studies
by Arthur Evans Westwell

A thesis submitted to the Graduate Faculty in partial fulfillment of the requirements for the degree of
DOCTOR OF PHILOSOPHY in Chemistry
Montana State University

Abstract:
An attempt was made to determine the effects on micellization of polar head modifications of decylpyridinium bromide. The differences in aggregation numbers of the surfactants studied are in general not large, and appear to be due more to interactions between polar heads and solvent than to interactions between polar heads.

The ideal optical characteristics of the Brice-Phoenix Differential Refractometer were investigated by means of a computer program and compared to the performance of an actual instrument and the description of its designers It was shown that the possibility of small errors in construction and alignment require an empirical calibration of the instrument rather than the designer's geometrical one, which is approximate at best.

Apparently anomalous results of light scattering by cetylpyridinixim chloride solutions were resolved by demonstrating the adsorption of this compound on glass filters. Unless precautions are taken, the phenomenon can be troublesome in light scattering work with surfactant solutions of low concentration.

SURFACTANT STUDIES

by

ARTHUR EVANS WESTWELL

A thesis submitted to the Graduate Faculty in partial fulfillment of the requirements for the degree

of

DOCTOR OF PHILOSOPHY

in

Chemistry

Approved:

E. W. Saunders
Head, Major Department

E. W. Saunders
Chairman, Examining Committee

R. Goering
Graduate Dean

MONTANA STATE UNIVERSITY
Bozeman, Montana

March, 1974

ACKNOWLEDGEMENTS

A good many people--parents and friends-- have given me much encouragement in the completion of this work. I especially want to thank Paul Jacobs, not only for preparing some of the compounds used in this study, but for the benefit of his opinions and experience at all stages of the research.

I am particularly grateful for a generous sabbatical year's leave which was made available through the action of Fr. Joseph D. Harrington and the Trustees of Carroll College. I would also like to acknowledge support from the National Science Foundation, which helped sustain this project.

My deepest thanks are for my advisor, Ed Anacker, for his limitless supply of encouragement and patience and, no less, for an introduction to Montana wilderness country.

TABLE OF CONTENTS

LIST OF TABLES

LIST OF FIGURES

ABSTRACT

An attempt was made to determine the effects on micellization of polar head modifications of decylpyridinium bromide. The differences in aggregation numbers of the surfactants studied are in general not large, and appear to be due more to interactions between polar heads and solvent than to interactions between polar heads.

The ideal optical characteristics of the Brice-Phoenix Differential Refractometer were investigated by means of a computer program and compared to the performance of an actual instrument and the description of its designers. It was shown that the possibility of small errors in construction and alignment require an empirical calibration of the instrument rather than the designer's geometrical one, which is approximate at best.

Apparently anomalous results of light scattering by cetylpyridinium chloride solutions were resolved by demonstrating the adsorption of this compound on glass filters. Unless precautions are taken, the phenomenon can be troublesome in light scattering work with surfactant solutions of low concentration.

PART I

Ring Substituent Effects on Decylpyridinium Bromide Micellization

INTRODUCTION

The concept of surfactant monomer aggregation in solutions is due to an explanation for the low osmotic activity and relatively high conductivity of soap solutions that was suggested by J. W. McBain in 1913 (1). The idea is now generally accepted that monomers consisting of nonpolar hydrocarbon chains attached to polar groups can aggregate to form colloidal size particles (micelles) in solutions of high enough concentration. If one measures a physical property of such a solution an abrupt change in the property is generally found to occur at what appears to be a characteristic concentration--the critical micelle concentration (CMC). It is probably more accurate to consider the CMC as a narrow concentration range in which the habit of the dissolved surfactant changes from mostly monomer to mostly micelle.

The general structure of the micelle is considered to be a cluster of the hydrocarbon chains with their polar heads exposed to solvent. When the surfactant monomer is ionic, the micelle will be a charged particle whose net charge depends upon association with oppositely charged ions from the solution (counterions). For small micelles, a spherical model seems likely (2-8). When the number of monomers per

micelle (aggregation number) is large, the spherical model appears inadequate and other shapes have been suggested such as rods and ellipsoids (6-10).

In the investigations of micelles which have followed McBain's original suggestion, one of the most fruitful techniques for determining aggregation numbers has been that of light scattering. The application of this method to surfactant studies stems from the work of Debye (11, 12), and has been developed to treat multicomponent systems of surfactant and electrolyte by a number of investigators (13-21). In this study aggregation numbers were determined by light scattering and with the equations of Anacker and Westwell (8, 22).

A number of factors that affect surfactant micelle size have been conclusively demonstrated. Aggregation numbers will decrease with a rise in temperature (9, 23), they will increase with increased length of the hydrocarbon chain (9, 23), and they are sensitive to the presence of counterions in solution. Micelle size of ionic surfactants can vary considerably according to the choice of counterion (8, 24), and generally will become larger with increased counterion concentration. In contrast, there seems to be little relationship between aggregation number and ions with

the same sign charge as the surfactant monomer (23, 25).

The nature of the polar head has also been recognized as an important factor in micelle formation, but this has not been thoroughly or systematically studied until recently. Other investigations in this laboratory have shown that approach of counterions to the charge center on a variety of ammonium-type polar heads can be sterically hindered by side chains, resulting in smaller micelles (26, 27). These studies have also indicated the importance of polar head-water interactions. Jacobs and Anacker have shown that aggregation numbers of pyridinium ring-decyl chain compounds depend upon the point of attachment of the chain to the ring (28). Micelles are smallest when the chain is on the ring atom bearing the greatest positive charge, and where it can produce the greatest hindrance to the approach of a counterion to that charge.

In addition to the steric and solvent effects, any factor that might enhance the close approach of polar heads would seem to increase the chances for larger micelles. Presumably the presence of counterions does this by helping reduce charge repulsion between neighboring polar heads, but there are several other possibilities.

Another means of reducing charge repulsion between

polar heads would be ionization of the polar head to produce an over-all neutral species. Veis and Hoer have made careful measurements of the pH of decyl- and dodecylammonium chloride solutions without added electrolyte (29). The sharp drops in pH observed at the CMC's correspond to the loss of protons from $-NH_3^+$ groups. It is also possible for an alkyl group attached to the 2 or 4 position of a pyridinium ring to lose a proton from the carbon adjacent to the ring (30). If this neutralization effect were important in contributing to micelle formation, a difference in aggregation number might be detected in a series of substituted pyridinium surfactants. Loss of the proton from an -OH group on a cationic polar head is another way in which charge neutralization might be effected.

Hydrogen bonding might be a possible link between polar heads that would promote micelle formation.

Hydrophobic bonding and Van der Waals attraction between alkyl groups on different polar heads have been suggested as factors in micellization (6, 27). These groups, however, could also be sources of steric hindrance.

Stead and Taylor have argued that increased delocalization of charges on polar heads would allow closer approach, and give as an example of this possible effect the lower

CMC's of 1-dodecyl-4-methoxypyridinium bromide and chloride compared to the unsubstituted dodecylpyridinium analogs (32). From measurement of base strengths it is known that alkyl groups can increase the electron density on the pyridine ring (31). Substitution at the 4 position is more effective than at the 3, and the base strength does not change as the group at the 4 position is varied through the series methyl, ethyl, i-propyl and t-butyl. Pyridinium surfactants with alkyl groups at different positions might have aggregation numbers reflecting a difference in charge delocalization. On the other hand, differences in micelle size for a series of alkyl groups at the same position should be due to other causes.

The pyridinium polar head is seen to be a particularly interesting and versatile one for investigation of the effects mentioned above. There is the possibility of various substituents at the different ring positions which might allow detection of steric effects as well as those due to charge delocalization and ionization. The planar structure of the group could also permit closer approach of polar heads than was possible with the ammonium-type surfactants of other comparison studies (26, 27). This might produce a greater sensitivity of aggregation number to some of the

factors depending upon polar head interaction.

Since chances of encountering insoluble materials are greater with increased hydrocarbon chain length, surfactants with a decyl group were chosed for this study. They were prepared as bromide salts not only because of the relative ease of preparation, but for the good aggregating power of this ion which was also the counterion of choice.

In addition to the determination of aggregation numbers of twenty different pyridinium-type surfactants, information was also sought from pH measurements, dye solubilization, and calculation of charge distribution on the substituted pyridinium ring.

EXPERIMENTAL

The light scattering measurements were carried out with a Brice-Phoenix Universal Light Scattering Photometer, Series 2000, with an attached chart recorder. Scattering and transmitted intensities were determined as average peak heights for several measurements of a sample, extrapolated back to zero time for the sample in the instrument. This was done because of a general drop of peak height with time, probably due to warming of the solution after it had been placed in the photometer.

All measurements were made with the same cylindrical scattering cell (Brice-Phoenix Catalog no. C-105).

Light of 435.8 nm was used in all determinations. Since one of the compounds studied (decyl 4-cyanopyridinium bromide) was visibly colored and absorbed more strongly at 435.8 nm than at 546.0 nm, scattering measurements were also made for this compound at the latter wavelength. The loss in scattering intensity due to use of a longer wavelength was greater than the intensity loss from absorption at the shorter wavelength, so these results were not used for determining the aggregation number. Instructions for the instrument indicated that no correction was required for

measurements of absorbing solutions unless absorption were much greater than that encountered in this case.

The scattering intensities used in the determination of aggregation numbers were measured at 90^{o}. For each sample intensities were also measured at 45^{o} and 135^{o} to check for dissymmetry in the scattered light. Dissymmetry was not detected in any of the samples measured, which meant that the scattering particles were small compared to the wavelength of the incident light.

Samples were prepared by adding weighed amounts of solvent to known weights of surfactant. The solvent consisted of 0.5 molal electrolyte (NaBr, NaCl, HBr, HCl) in water. The water used for these solutions was obtained from reverse osmosis and was then distilled from alkaline permanganate solution. The electrolytes used were reagent grade. A series of solutions for a compound usually consisted of 12 samples ranging from about 3×10^{-3} to 7×10^{-2} molal in surfactant concentration.

The samples were introduced into the scattering cell by filtration through an ultrafine fritted glass filter under nitrogen pressure. Solvent was measured first, and then several samples of the least concentrated surfactant solution were run through the filter until successive samples

gave consistent light scattering results (see Part III).

Cell and filter were cleaned beforehand with hot chromic acid solution and rinsed thoroughly with doubly distilled water. The filter was also washed with ammonia solution after treatment with the acid. Absence of dust in the cell was determined from scattering measurements with water taken directly from the still.

Temperature was controlled by keeping the entire room at 25°. Temperature within the photometer would rise 5 to 6 degrees during the series of measurements for one surfactant.

Refractive index measurements were made on unfiltered portions of the same solutions used for light scattering. Only solutions above the critical micelle concentration were measured and compared with the electrolyte solvent. The instrument used was a Brice-Phoenix Differential Refractometer, Model BP-2000-V. Its characteristics are discussed in Part II. The purpose of these measurements was to determine the variation of solution refractive index with surfactant concentration, a quantity required in the calculation of aggregation numbers. In the Brice-Phoenix refractometer this is done by finding the amount of deflection of a slit image that occurs when solutions of different surfactant concentration are compared to solvent in a two section cell.

The relationship of image deflection to refractive index increment for the instrument used was found by empirical calibration. A series of NaCl solutions of accurately known molality was prepared, and the refractive index of each solution was calculated from the refractive index data of Kruis (33). A least squares treatment of Kruis's data gave the following relationship between Δn, the difference between refractive index of solvent and solution, and the NaCl molality (m)

$$\Delta n \times 10^3 = 0.00281 + (10.6203)m - (0.817256)m^2 + (0.155446)m^3$$

This expression was used to calculate the refractive index increment of the NaCl solutions prepared for the instrument calibration. When slit image deflections (Δd) were measured for these solutions, it was apparent that there was not the strict proportional relationship between Δn and Δd that has been claimed by the instrument designers (see Part II). A least squares treatment of the experimental data gave this relationship

$$\Delta n = (9.9737 \times 10^{-4})\Delta d - (1.230 \times 10^{-6})(\Delta d)^2$$

Temperature control for solutions in the refractometer is achieved by circulating water from a constant temperature bath through the metal housing containing the sample cell. After introducing solution into a cell compartment, from 6 to

7 minutes is required for temperature equilibration. A constant reading for the slit image position is not obtained until equilibration has been achieved.

A problem that occurred persistently in the first several series of compounds measured was flow of surfactant solution to the top of the refractometer cell. This appeared to be happening in the corners of the cell compartments, and did not appear to be taking place in the compartment containing solvent. This solution flow seemed to be causing concentration changes either through evaporation at the top of the cell, or by mixing with solvent. When liquid was visible on the top edges of the cell, deflection readings became erratic and inconsistent with prior measurements. This problem was eliminated by removing the cell mounting from the instrument and dipping the top of the cell in melted paraffin. Pressing on the top of the soft wax at the top of the cell with a glass plate produced a smooth flat surface which gave a good seal with the cell cover glass. The paraffin coating prevented solution from reaching the top of the cell.

Each time fresh solution was added to one of the cell compartments the compartment was rinsed several times with the solution to be used.

A Cary Model 14 Recording Spectrophotometer was used

in measurements of dye solubilization. The dye used was Orange-OT (OOT), originally prepared by P.T. Jacobs for other investigations (34). For determination of solubilization efficiency, solutions of surfactant in 0.5 m NaBr were prepared as in the light scattering work. To these solutions were added small amounts of OOT in excess of what would ultimately be solubilized. The solutions were sealed in water-tight vials and shaken in a constant temperature bath for five days at 25°. They were then allowed to settle out for two days in the water bath without shaking. Samples for analysis were withdrawn with a hypodermic syringe. In order that all absorption measurements would fall on the same instrument scale, solutions of greater OOT concentration were diluted quantitatively. This was done with a 2% solution of decylpyridinium bromide in 0.5 m NaBr to ensure that all OOT originally solubilized would remain in solution. Spectral scans were made for all samples run, and a maximum absorbance for OOT was found at 498 nm in all cases.

The extinction coefficient was determined for OOT in 2% solutions of various surfactants in 0.5 m NaBr. Small measured amounts of 3.13×10^{-2} molar OOT in acetone were added to weighed amounts of surfactant solutions with a microliter syringe to give OOT solutions of known molality.

Absorbances were measured at 498 nm, which again corresponded to maximum absorbance for all solutions measured.

The pH measurements were made on several sets of solutions of different surfactants above the CMC. The instrument used was a Radiometer pH Meter 4 d with glass and calomel electrodes. Consistent and stable readings were not obtained with the surfactant solutions, possibly due to adsorption of surfactant on the membrane of the glass electrode (see Part III). Another possible source of trouble with these measurements might have been changes in the nature of the surfactant solution due to high chloride ion concentration at the interface with the KCl solution of the calomel electrode.

The compounds used in this study were in general prepared by reacting equimolar amounts of n-decyl bromide and the appropriate substituted pyridine to form substituted decylpyridinium bromide salts. Starting materials that were visibly colored were vacuum distilled before use. Initially these syntheses were carried out by refluxing the two reactants together under a nitrogen atmosphere for 10 to 20 minutes. This usually led to rapid and vigorous reactions and the development of much dark color in the reaction mixture. When the reaction appeared to be complete the mixture

was cooled and impure product solidified as a hard waxy mass. Complete solidification could occur in a few minutes at room temperature, overnight in the refrigerator, or could require several weeks of refrigeration. When reactions were carried out in this manner, lower reactivities were apparent for pyridine compounds with substituents in the 2 position.

The products were recrystallized from acetone, ethanol or mixtures of these two solvents. Refrigeration was usually required. In some cases addition of diethyl ether precipitated the product from solution; in other cases addition of ether caused the product to form a separate liquid layer. Recrystallizations were carried out until there was no perceptible color remaining in the product. An exception was the derivative of 4-cyanopyridine, which was bright yellow. The sequence of recrystallizations for some compounds required from 2 to 3 months. The purified products were vacuum dried over P_4O_{10}. Several of the compounds were markedly hygroscopic and subsequent handling of them was done in a nitrogen filled glove bag.

It was found that cleaner products could be obtained if the reactants were dissolved in ethanol and refluxed under nitrogen for 3 to 5 days. After this period, ethanol and excess reactants were removed by vacuum distillation and the

product was solidified by cooling. Further treatment of product was carried out as before, but only 5 or 6 recrystallizations were usually required to give a colorless product.

The decylpyridinium bromide monohydrate was from a lot prepared by P. T. Jacobs for a separate investigation (34). The compounds with methanol groups at the 2, 3, and 4 positions of the pyridinium ring were originally made by M. O. Gunsch and were recrystallized and reanalyzed for this investigation. The 3 and 4 methoxymethyl compounds were prepared by P. T. Jacobs for this work.

Composition of the compounds was checked by gravimetric analysis of the bromide content. A summary of the results is given in Table 1 along with a list of symbols used to identify the various surfactants studied.

There were several interesting failures among the attempted syntheses. No reaction could be detected with 2-bromo, 2-cyano, or 2-ethoxypyridine. Reaction with 2-n-propylpyridine yielded a white crystalline product which did not foam in water solution. Bromide analysis and the NMR spectrum suggest that this was 2-n-propylpyridinium hydrobromide. Reaction occurred between decyl bromide and 2-ethanolpyridine to produce a highly viscous material which

TABLE 1

BROMIDE ANALYSIS OF SURFACTANTS

Surfactant	Symbol	%Br Calculated	%Br Found
Decylpyridinium bromide·H_2O	DPB	25.10	25.11
Decyl-2-methylpyridinium bromide	2M	25.42	25.41
Decyl-3-methylpyridinium bromide	3M	25.42	25.47
Decyl-4-methylpyridinium bromide	4M	25.42	25.43
Decyl-2-ethylpyridinium bromide	2E	24.34	24.35
Decyl-3-ethylpyridinium bromide	3E	24.34	24.33
Decyl-4-ethylpyridinium bromide	4E	24.34	24.36
Decyl-2-methanolpyridinium bromide	2MOL	24.19	24.18
Decyl-3-methanolpyridinium bromide	3MOL	24.19	24.19
Decyl-4-methanolpyridinium bromide	4MOL	24.19	24.00
Decyl-3-propanolpyridinium bromide	3POL	22.30	22.28
Decyl-4-propanolpyridinium bromide	4POL	22.30	22.36
Decyl-3-methoxymethylpyridinium bromide	3MOM	23.21	23.20
Decyl-4-methoxymethylpyridinium bromide	4MOM	23.21 (compound unstable)	-
Decyl-3-cyanopyridinium bromide	3CN	24.56	24.55
Decyl-4-cyanopyridinium bromide	4CN	24.56	24.52
Decyl-3-bromopyridinium bromide	3BR	21.07	21.10
Decyl-3-hydroxypyridinium bromide	3OH	25.26	25.22
Decyl-4-t-butylpyridinium bromide	4TB	22.42	22.40
Decyl-4-ethanolpyridinium bromide	4EOL	23.21	23.12

resisted all attempts at crystallization. Since direct distillation of this pyridine compound can produce 2-vinylpyridine (35), it is possible that polyvinylpyridine was produced in the reaction. A reaction also occurred between decyl bromide and 2-propanolpyridine. Bromide analysis and investigation by P. T. Jacobs indicated that the product formed had the structure given in Figure 1.

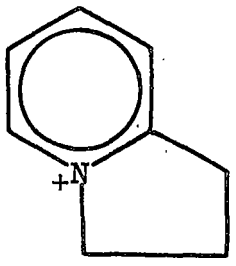

Fig. 1.--Possible Product from 2-propanol Reaction

Reactions with 4-n-propylpyridine and 4-isopropylpyridine appeared to give satisfactory yields of surfactant, but no means were found of recrystallizing and purifying these products for further use.

DISCUSSION

Aggregation numbers for the surfactants studied were calculated from the equations of Anacker and Westwell for surfactant solutions with added electrolyte (8, 22). Scatterin data are treated in accordance with an equation which can be written as

$$Km_2'/R_{90} = A + Bm_2' + \ldots\ldots$$

where

$K = 2\pi^2 n^2 n_2'^2 V^o / L\lambda^4$

$A = 4N\{(2N - fp)^2 + pf^2\}^{-1}$

$B = pA(2m_3)^{-1}\{(1 + p)N^{-1} - A\}$

N = aggregation number

p = effective micellar charge

$f = (\partial n/\partial m_3)_{m_2'} / (\partial n/\partial m_2')_{m_3}$

m_2' = molality of micellar salt (total surfactant molality minus CMC)

R_{90} = Rayleigh ratio at 90^o scattering angle ($=3\tau/16\pi$)

n = solution refractive index

$n_2' = (\partial n/\partial m_2')_{m_3}$

m_3 = molality of supporting electrolyte

V^o = volume of solution (cm^3) contining 1 kg water

L = Avogadro number

λ = wavelength (cm) in vacuo of light used

τ = turbidity of solution minus turbidity at CMC

Primed quantities designate molalities in terms of monomer units.

The first equation is based on these assumptions: there is no depolarization of scattered light at 90°; micelles are small compared to λ (there is no dissymmetry); R_{90} represents scattering in excess of that at the CMC; unaggregated surfactant (concentration assumed equal to CMC) can be considered part of the supporting electrolyte.

Equations relating the scattering data to the effective micelle charge and the aggregation number are

$$p = \{2fm_3B + (8m_3B)^{\frac{1}{2}}\}A^{-1}(2 - fA)^{-1}$$

$$N = p(p + 1)A(2m_3B + pA^2)^{-1}$$

If p = 0, N is not calculated from the second equation but from the definition of A. The quantities A and B are determined experimentally as the intercept and slope respectively of a Km_2'/R_{90} vs. m_2' plot and are then used to calculate values of p and N. A computer program is available for performing these calculations. This program calculates the CMC, A^{-1}, N and p for a least squares linear plot of Km_2'/R_{90} vs. m_2'. A^{-1} is an approximation (uncorrected for charge) of the aggregation number.

It was intended that all light scattering work be

done with 0.5 m NaBr as solvent, however in some instances chloride rather than bromide solutions were used. This was done either because of insolubility of a surfactant in 0.5 m NaBr (3OH, 4TB), or to allow comparison of aggregating abilities of the bromide-insoluble compounds with those of some of the other surfactants.

When the counterion of the added electrolyte was chloride, the changes of solvent and solute refractive indices with concentration were calculated as described by Anacker and Ghose (8). When calculations were made for a family of isomers the surfactant refractive index gradient used was usually an average of those determined experimentally for the individual compounds. An exception to this was made for the case of the rather different isomers 3MOM and 4EOL where the measured gradients are not very close to the same value. An average was not used for 3MOM and 4MOM since data for 4MOM are not considered very reliable.

Calculated aggregation numbers are given in Tables 2 and 3 along with the CMC's determined from light scattering and from dye solubilization. A key to compound symbols has been given in Table 1. Aggregation numbers in parentheses are not corrected for charge. In some cases only a value uncorrected for charge (A^{-1}) is available. This occurs when

TABLE 2

AGGREGATION NUMBERS OF SURFACTANTS IN 0.5 m NaBr AT 25°

Surfactant	Aggregation Nr.	CMC x 10^3 Scattering	CMC x 10^3 Solubilization
DPB	50 (47 ±0.5)*	11.1	11.2
2M	45 (43 ±0.2)	10.2	10.2
3M	43 (42 ±0.1)	8.9	9.2
4M	45 (43 ±0.2)	8.6	9.3
2E	40 (38 ±0.3)	7.6	8.0
3E	44 (42 ±0.2)	7.0	7.8
4E	43 (42 ±0.3)	6.9	7.6
2MOL	58 (57 ±0.3)	8.9	6.6
3MOL	51 (49 ±0.5)	10.6	8.8
4MOL	52 (49 ±0.2)	9.8	9.0
4EOL	47 (44 ±0.5)	10.2	10.3
3POL	36 (35 ±0.2)	9.0	9.4
4POL	40 (38 ±0.9)	8.8	8.6
3MOM	37 (36 ±0.2)	9.4	9.5
4MOM	(38 ±0.5)	2.0	-
3CN	(50 ±0.5)	10.5	13.0
4CN	(67 ±0.7) (95 ±0.8)	6.2 11.6	- -
3BR	(56 ±0.5)	8.0	8.0

* Values in parentheses are uncorrected for charge. Uncertainties are for least squares determination of A^{-1}.

TABLE 3

AGGREGATION NUMBERS OF SURFACTANTS IN VARIOUS SOLVENTS AT 25°

Surfactant	Aggregation Number	CMC x 10^3 (Scattering)
Solvent = 0.5 m NaCl		
4MOL	(37 ±0.1)*	15.4
3BR	(33 ±0.0)	14.6
4CN	13 (11 ±0.3)	36.0
4TB	36 (34 ±0.4)	7.9
3OH	50 (48 ±0.8)	6.7
Solvent = 0.5 m HBr		
3E	45 (44 ±0.2)	8.2
3MOL	49 (47 ±0.4)	13.5
3POL	35 (34 ±0.4)	12.2
Solvent = 0.5 m HCl		
3OH	(44 ±0.4)	9.8

* Values in parentheses are uncorrected for charge. Uncertainties are for least squares determination of A^{-1}.

the plot of scattering intensity vs. surfactant concentration shows concave upward curvature above the CMC, an effect which is generally believed to result from polydispersity in micelle size and/or an increase in size with concentration (6, 8, 10, 24). The charge-uncorrected values represent lower limits for aggregation numbers, and in most cases where charge-corrected values are available for comparison the uncorrected values are only one or two units lower. A summary of experimental data, and typical data plots, are given in appendix B.

The very different aggregation numbers calculated for two separate determinations of 4CN in 0.5 m NaBr arise from the anomalous behavior of this compound. In a concentration range that appears to start at the CMC, samples of this compound gave markedly higher scattering than was consistent with most of the data for 4CN. Consecutive samples of a single solution in this range , after filtration into the scattering cell, did not produce the same scattering. After two or three different solutions gave these erratic results, subsequent solutions showed the regular and uniform increase of scattering with concentration that is expected for a scattering curve. Unfiltered portions of the oddly behaving solutions showed no anomalies when refractive indices were

determined. The phenomenon is specific for 4CN since it occurs with no other compound studied and was very evident in both determinations of 4CN in 0.5 m NaBr, and to a lesser extent in an attempt to determine the aggregation number of 4CN in 0.5 m NaCl. Since the material is known to be adsorbed onto the filter (see Part III), a possible explanation of this behavior is that with solutions above the CMC some of the adsorbed surfactant may be attracted back into solution in micellar form. The disparity in the two aggregation numbers determined for this compound in 0.5 m NaBr can be attributed to the lack of reliable scattering data in the neighborhood of the CMC. It is safe to say only that micelles of 4CN are probably large compared to the rest of those studied in 0.5 m NaBr.

The instability in air of 4MOM and the lack of consistent bromide analyses put the results for this compound in question. There is nothing apparently unusual in the aggregation number, but the value determined for the CMC is notably lower than that for any other compound in the series.

When solutions of 4MOL and 4EOL were prepared, a small amount of insoluble material was visible in the samples of both compounds. After filtration the solutions were clear and the low scattering from samples below the CMC

indicated that no colloidal or larger particles were present. This implies that the true surfactant concentrations in these solutions were lower than the calculated values because of an insoluble impurity in the compounds. Calculations for 4EOL on the assumption that true concentrations were 10% less than those originally calculated revised the aggregation number from 47 to 42. The 10% assumption is a considerable exaggeration of the amount of impurity, and a more accurate adjustment of concentrations would probably not reduce the calculated aggregation number by a significant amount. The bromide analyses of the two compounds in question are low, and the differences between the analytical and the calculated precents are larger than for any of the other compounds studied (Table 1). If the analytical results are accurate measures of the amounts of surfactant in these preparations, the percent of impurity would be 0.4% and 0.8% respectively for 4EOL and 4MOL.

The small differences in aggregation numbers accompanying the substitution of different groups on the ring show that the various effects suggested in the Introduction can play only a small role at most in determining micelle size for the compounds studied. This is in contrast to other influences that have been studied by light scattering such as

choice and concentration of counterion, length of hydrocarbon tail, and large variations in polar head structure.

The influence of counterion has been investigated by Anacker and Ghose in a study of hexadecylpyridinium bromide (8). For 0.2 m sodium salts of IO_3^-, F^-, Cl^-, BrO_3^- and Br^- as supporting electrolytes, the aggregation numbers were 101, 117, 129, 130 and 2140 respectively. In the present work the dependence upon counterion identity can be seen in the lower aggregation numbers found for 4MOL and 3BR when determined in 0.5 m NaCl as compared to the values for 0.5 m NaBr.

Anacker has shown (5) that the aggregation number of hexadecylpyridinium chloride increases with chloride concentration from a value of 95 in 0.0175 M NaCl to 135 in 0.730 M NaCl.

Aggregation numbers were determined by Jacobs, Geer and Anacker (34) for a series of alkyl pyridinium surfactants with chains of 9 to 14 carbon atoms. The aggregation numbers were 35, 49, 64, 77, 98 and 136 respectively in NaBr solutions.

The extent to which variation in polar head structure can influence micellization can be seen in some of the results of Geer, Eylar and Anacker (26) from decylammonium bromide and some of its derivatives. With no substitution

on the ammonium group, the aggregation number in 0.5 m NaBr is 1100. Aggregation numbers for different substitutions were found to be: 670 (methyl), 69 (dimethyl), 48 (trimethyl), 65 (diethyl) and 37 (triethyl).

In comparison to these other results, the differences in micelle size that appear in this study are minute and must be interpreted with caution. It is evident that 3OH has superior aggregating ability compared to the other compounds. Although this compound is not soluble in 0.5 m NaBr, the aggregation number for 3OH in 0.5 m NaCl is substantially larger than that for the compounds that were determined in both solvents. It also seems clear that the presence of an alkyl group leads to a small decrease in size, although it is not clear whether or not the micelle size depends upon the size of the group in going from methyl to ethyl. There is no evidence that the position of such a group on the ring has an effect on aggregation number. The only cases where ring position seems important are with 2MOL which shows a markedly larger size than 3MOL and 4MOL, and with 3CN and 4CN. This latter compound has proved to be highly anomalous in its behavior and is not reliable for making comparisons.

There appears to be a definite trend in aggregation number according to the size of substituents containing -OH

groups. If one considers the series 3OH; 2-, 3-, and 4MOL; 4EOL; and 3- and 4POL there is a consistent decrease in aggregating ability. Another relationship that appears associated with the -OH group is seen when comparisons are made between groups of close to the same size. Considering the -OH group to be approximately the same size as $-CH_3$, one can compare hydroxy vs. methyl, and methanol vs. ethyl. In both cases the compounds with -OH groups have the larger micelles. There is also the comparison of 4EOL with its isomers, 3MOM and 4MOM. Again the compound with the hydroxy group is the larger.

There are not enough data from other types of groups to detect trends. A cyano group at the 3 position does not appear to change the aggregation number, while a bromine at this point seems to cause a slight increase. Insolubility of 4TB in 0.5 m NaBr prevents a direct comparison with the other alkyl substituted compounds. Since the aggregation number of 4TB in 0.5 m NaCl is much the same as for 3BR and 4MOL, it appears that this compound is not exceptional in its aggregating ability. The very low and very unreliable aggregation number for 4CN in NaCl solution is another instance of the odd behavior of this compound.

From the determinations of micelle size it is possible

to conclude that hydrophobic bonds or Van der Waals forces due to alkyl side chains do not facilitate micelle formation with the compounds studied. Because of the general insensitivity of micelle size to the position of a particular group on the ring, it also appears that steric hindrance of counterion approach is not taking place. The near equality of aggregation numbers for compounds with a group at the 3 or the 4 position indicates that differences in charge delocalization are not great enough to affect micellization of these compounds. The possibilities of polar head neutralization by ionization are discussed below in connection with pH measurements. Of the effects on micelle formation that were suggested in the Introduction, there remains the possibility of hydrogen bonding between -OH groups on adjacent polar heads.

It is tempting to ascribe the relative tendency to large size for hydroxy-containing compounds to this cause. It is difficult, however, to see why this would be more effective for 2MOL than for 3MOL, and why it could be as effective for 4MOL as for 3MOL unless polar heads can easily incline toward one another. The high aggregating ability of 3OH would demand a rather close approach of polar heads if it is dependent upon hydrogen bonding. Hydrogen bonding

cannot be ruled out as a factor in the results of this investigation, but it could only account for the tendency to larger size noted, and not for the decrease in size that is connected with the length of the hydrocarbon part of the attached groups.

The extinction coefficient for OOT was found from the slope of a Beer's Law plot for OOT dissolved in 2% solutions of various surfactants in 0.5 m NaBr. The results of these measurements are plotted in Figure 2, and with the exception of the data for 4MOL, all points fall close to a single straight line. A least squares calculation gives the slope of this line as 1.77×10^4 kg/mole cm. This is identical to the extinction coefficient determined by Jacobs and Anacker for OOT in a series of decyl surfactants with various non-pyridinium cationic heads (36). The coefficient for OOT in 4MOL solution was found to be 1.57×10^4 kg/mole cm. Measurements were made of the absorbance of OOT in several series of surfactant-NaBr solutions saturated with the dye. OOT molalities were calculated with the extinction coefficient values reported above. The slope of a dye molality vs. surfactant molality curve is the solubilization efficiency in terms of moles of dye solubilized per mole of surfactant monomer. These curves appeared linear within experimental

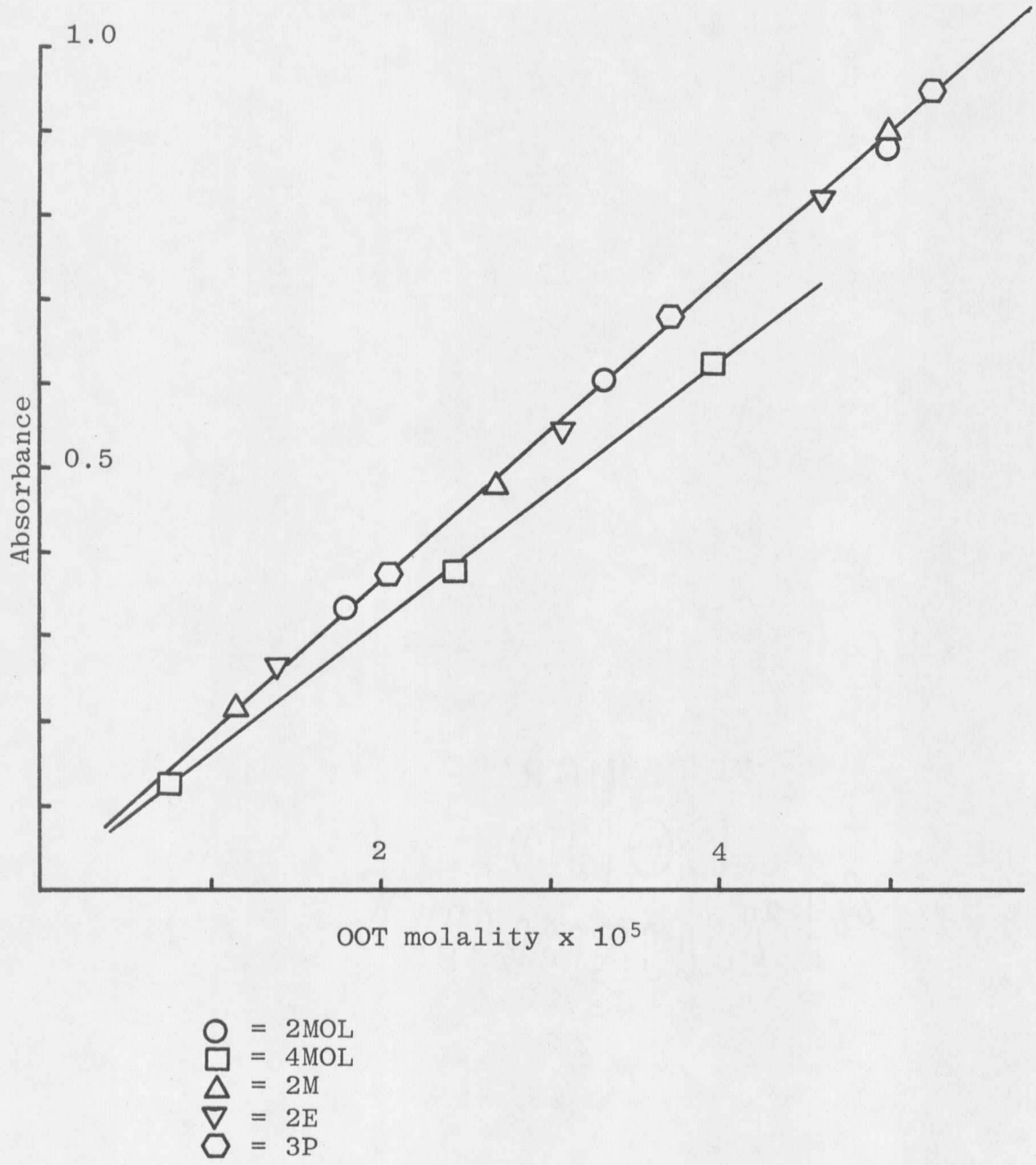

Fig. 2.--Beer's Law Plot of OOT in Different Surfactants

error for most of the series measured. A drop in solubilization efficiency at the highest surfactant concentrations used appeared to occur for 3POL, 4POL and perhaps for 4EOL as well. Slopes were determined by least squares for all surfactants, with the aberrant points for the above compounds excluded from the calculations of best-straight-lines. Intercepts of these curves with the surfactant concentration axis are the CMC values reported in Table 2.

Jacobs and Anacker have shown that solubilization of the dye OOT depends in large part on the size of micelles formed by a series of ammonium-type surfactants (36). In addition, increased amount of hydrocarbon character on the polar heads was correlated with increased solubilization efficiency. Since the micelles were much the same size for the compounds investigated in this study, dye solubilization measurements were made to see the effects of the variation in polar heads. There is some confirmation of increased solubilization accompanying the increase in hydrocarbon nature of some of the pyridinium heads. From Table 4 it is seen that the highest solubilization efficiencies were obtained for the polar heads with alkyl groups in the 2 position. This effect does not extend to the case in which there is a methanol group at this point. Since groups at

TABLE 4

SOLUBILIZATION EFFICIENCIES OF SURFACTANTS IN 0.5 m NaBr

Surfactant	Solubilization Efficiency x 10^3 (moles OOT/mole surfactant monomer)
DPB	5.2
2M	7.1
3M	5.4
4M	6.1
2E	7.4
3E	6.1
4E	6.3
2MOL	6.1
3MOL	5.6
4MOL	3.4
3POL	5.4
4POL	6.1
3CN	5.9
3BR	6.3
3MOM	5.8
4EOL	5.8

the 2 position of the ring are close to the hydrocarbon core of the micelle, these results support the idea that dye solubilization occurs principally within the core or near its surface rather than in the outer region of the polar heads. Since alkyl groups at the 3 and 4 positions do not contribute notably to solubilization efficiency, there is also some support for a model of the micelle in which the pyridinium rings are oriented at nearly right angles to the core boundary.

The slight indication that solubilization efficiency may drop off with increased concentration for 3POL, 4POL and 4EOL is a subject for further investigation. The case of 4MOL cannot at this point be accounted for. Solubilization of OOT is much less in solutions of this compound, and the dye showed about a 12% lower extinction coefficient than it did in solutions of the other surfactants used.

The results of pH measurements, as mentioned in the Experimental section, were generally inconclusive. Surfactants tested in 0.5 m NaBr solution were: 2MOL, 3MOL, 4MOL, 2M, 3M, 2E, 3MOM, 3POL, 3CN and 3BR. Solutions of 3OH, 4MOL and 3BR were measured in 0.5 m NaCl. Some consistency was obtained with the solutions of 3OH in NaCl. Solutions of this compound above the CMC showed pH values of 3.5,

3.4 and 3.3 with increasing surfactant concentration compared to 0.5 m NaCl solvent which measured 5.8. The other surfactant solutions were too similar to the solvent to prevent any pH difference from being obscured by fluctuations in the instrument readings. These fluctuations did not allow conclusions about the possibility of proton loss from alkyl side chains or -OH groups on polar heads except in the case of the definitely acidic 3OH. Another attempt to detect such an effect was made be determining the aggregation numbers of 3E, 3MOL and 3POL in 0.5 m HBr as well as in 0.5 m NaBr. If proton loss were making a significant contribution to micellization, aggregation numbers should be smaller in the acid solution. No significant differences were found for these compounds in the two solvents. When micelle size was determined for 3OH in 0.5 m HCl there appeared to be at least a small drop in the aggregation number from 50 in NaCl to about 44 in HCl. This indicates that self neutralization of a pyridinium polar head can play a role in determining micelle size.

Hückel molecular orbital (HMO) calculations were performed to discover how the positive charge might be distributed on the six atom ring which is the pyridinium polar head. The effect of substitution at various positions was

included by assuming an inductive effect at each of the different ring carbons in turn. It was assumed that the nitrogen atom in the ring was also subject to an inductive effect from the attached decyl chain. For purposes of these calculations the effect of the decyl chain was assumed equal to that of a methyl group. In addition to the calculations based on the inductive model for a substituent, HMO hetero-atom treatments were performed for -OH and -Br attached to the 3 position of the ring. Both of these groups were treated as atoms contributing two pi electrons to the seven atom system. Numerical values for the parameters used in both sets of calculations are given in Table 5.

TABLE 5

HMO PARAMETERS

Coulomb Integral	Bond Integral
$h_{N^+} = 2.0$	$k_{CN} = 1.0$
	$k_{CC} = 1.0$
$h_{Br} = 1.5$	$k_{C-Br} = 0.3$
$h_{OH} = 0.6$	$k_{C-OH} = 0.7$
$h_C = -0.5$*	$k_{C-Me} = 0$*
$h_X = +0.5$*	$k_{C-X} = 0$*

* inductive model
auxiliary inductive parameters: $h_C = 0.1h_{N^+}$, $0.05h_{OH}$, $0.05h_{Br}$

Except for h_X, k_{C-X}, h_{OH} and k_{C-OH} the values of Table 5 are taken from Streitwieser (37). The -OH values are from Yonezawa, Nagata, Kato, Imamura and Morakuma as given by McGlynn, Vanquickenborne, Kinoshita and Carroll (38). The h_X and k_{C-X} values are for an inductive effect assumed equal in magnitude to that of the methyl group but opposite in direction.

Results of the calculations are given in Figures 3 and 4. The numbers given represent the calculated charges associated with each ring atom and heteroatom substituent. In all cases R represents the decyl chain. Not included are the results of other calculations with the inductive model for a range of h_C and h_X values. The same general effects of substitution were obtained as those illustrated in Figure 3, with the magnitudes of the effects varying with the magnitudes of h_C and h_X.

The results of the HMO inductive model calculations indicate that about half of the positive charge remains on the nitrogen regardless of the substituent or its position on the ring. The rest of the charge is distributed somewhat differently depending upon the type of substituent group. For an electron donating group the charge tends to accumulate at the point of attachment to the ring, for an electron

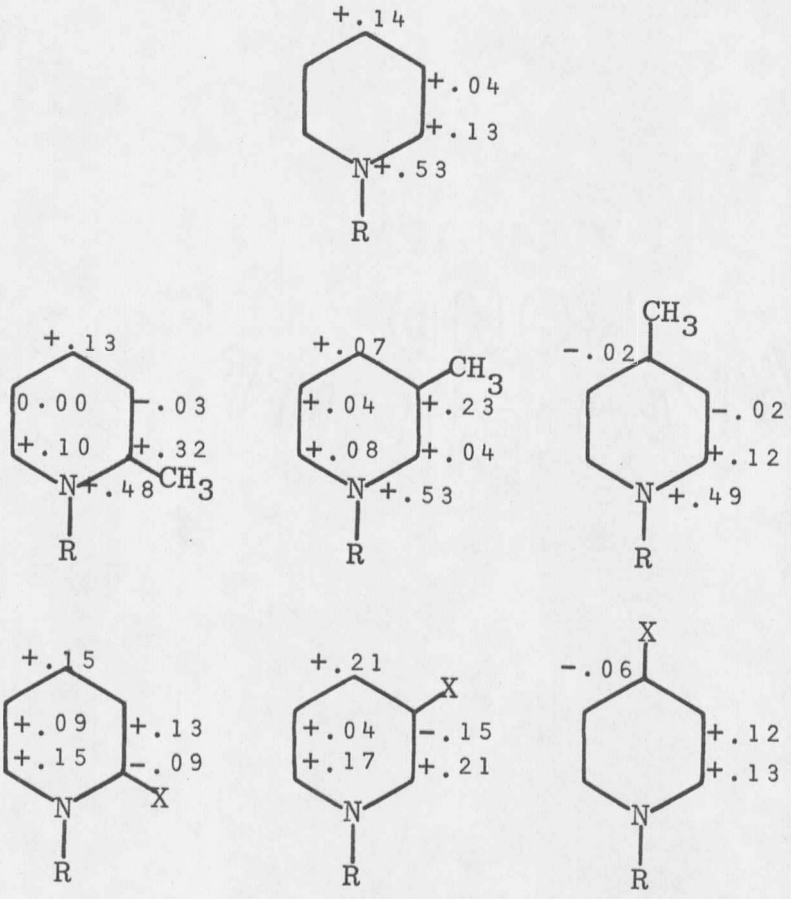

Fig. 3.--Calculated Polar Head Charges: Inductive Model

Fig. 4.--Calculated Polar Head Charges: Heteroatom Model

withdrawing group the charge is more evenly distributed about the ring.

The heteroatom models for 3OH and 3BR show charge distributions on the rings which are not greatly different from that on the unsubstituted ring, although 3OH and 3BR show a distinct difference in aggregating ability (Table 3). It does not appear that charge distribution effects of the magnitude of those predicted by these calculations are important in determining micelle size for the compounds studied. If charge delocalization is important in promoting close approach of polar heads, it is probably at smaller distances than those between heads in the micelles of this study. A more important factor is probably the closeness of approach of counterions to the charge center.

A simple model of the small micelles formed by the compounds studied can be constructed by assuming that a spherical hydrocarbon core, equivalent to a small drop of decane, is formed by the decyl chains of the surfactant monomers. For an aggregation number of 45 and a density for decane of 0.73 g/cm^3, the core radius is found to be 15 Å. This corresponds reasonably well to a calculated length of 13.2 Å for an extended decyl chain. If the 45 polar heads are distributed uniformly over the surface of the shere, the

nitrogen atoms of adjacent polar heads would be at a distance of about 8.5 Å from each other. This suggests that for the size of micelle encountered in this study close approach of polar heads is neither likely nor required, and effects due to close approach should not have great significance. It is still possible that delocalization of charge and bonding between hydrocarbon side chains might show detectable effects if large non-sherical micelles were studied such as those formed by hexadecylpyridinium bromide in NaBr (8).

This simple picture of the micelle indicates that polar heads could easily adopt an orientation that would allow hydrogen bonding between methanol groups on adjacent heads for 2MOL and 3MOL, although it does not seem that 2MOL would be especially favored. If the polar heads can be inclined away from a perpendicular orientation to the core surface by only about 30^{o}, the methanol group of 4MOL could achieve practically the same position as that on a 3MOL head that is not inclined. Hydrogen bonding would seem to be a possibility for all three methanol-substituted compounds. Because of the apparent distance between polar heads, hydrogen bonding does not seem a factor likely to contribute to the aggregating ability of 3OH, which was the greatest of the compounds studied. The role of hydrogen bonding between

polar heads can not be determined from the evidence at hand.

There is no direct indication that the relatively small variations in aggregation number apparent in this study are due to interactions between polar heads. It is also possible that the determining factors involve polar heads and solvent instead.

An attractive explanation of the action of side chains in reducing micelle size involves the amount of solvent structure ("icebergs") that can form around hydrocarbon groups in water solution. It has been argued that the process of micellization is promoted by the entropy increase obtained when water structure is disrupted by hydrocarbon chains leaving their solvent environment to form micelles (41, 42). Anacker and Ghose (8) have correlated the aggregating abilities of anions in hexadecylpyridinium and dodecyltrimethylammonium surfactant solutions to their abilities to disrupt water structure. On this basis it seems likely that anything that would contribute to the formation of "icebergs" at the surface of the micelle would also inhibit micelle formation. Alkyl side chains on polar heads might promote this effect. Such a possibility may be related to the fact that compounds prepared with alkyl groups on the ring tended to be hygroscopic and the ethyl compounds were

markedly more hygroscopic than the methyl ones.

Appart from the ionization effect, it is difficult to see how the presence of an hydroxy group could promote aggregation by interaction with solvent. The most likely interaction would seem to be hydrogen bonding with water with a concomitant increase in water structure. Unless this structure were more susceptible to being broken in micellization than that around an alkyl side chain, there would be no special reason for the greater aggregating ability of the compounds with hydroxy side chains.

SUMMARY

Aggregation numbers of twenty different decylpyridinium surfactants showed only minor variations. Two trends appear in the results. The presence of an alkyl side chain on the pyridinium ring seems to lower the aggregation number, and the presence of an hydroxy group appears to oppose this trend.

There were no general effects on aggregation numbers that were traceable to the position of substituent groups on the pyridinium ring. Perhaps because of the small size of the micelles encountered, there was no detectable contribution to micellization from bonding between alkyl groups on the heads or reduced repulsion between heads from charge delocalization. Such effects might become significant with larger non-spherical micelles in which polar heads would be forced closer together. There is evidence that ionization of polar heads can be a factor in determining micelle size.

The opposing trends noticed in the series of compounds studied may be due on the one hand to increased water structure around alkyl side chains on the ring, which could inhibit micellization. On the other hand, the tendency toward increased aggregation number that is associated with

the presence of -OH groups might be due in part to hydrogen bonding between polar heads or to some type of interaction of -OH groups with solvent, including ionization.

Solubilization determinations of the dye OOT with a number of the surfactants indicated a special role is played by alkyl substituents at the 2 position of the ring. This is probably due to the proximity of these groups either to the charge center on the nitrogen, or to the hydrocarbon interior of the micelle, or to both.

PART II

Differential Refractometer:

Optical Characteristics

INTRODUCTION

An important empirical quantity necessary for the calculation by light scattering of micelle aggregation numbers is the refractive index increment dn/dc. The refractive index of the solution is n, and the total surfactant concentration minus the critical micelle concentration (CMC) is c. In actual practice, the slope is calculated at the CMC for a Δn vs. surfactant concentration curve and this quantity is used for dn/dc. To a first approximation the aggregation number is inversely proportional to the square of this term; hence it is important to have the best possible values for this quantity, especially when small differences in aggregation numbers are being compared as in Part I

The instrument used to obtain refractive index data for the light scattering work discussed in the preceding part is a Brice-Phoenix Differential Refractometer, Model BP-2000-V. A diagram of the optical system of this instrument is given in Figure 5. Light from a mercury vapor lamp (L) passes through a monochromatic filter (F) and illuminates a slit (S). Light from the slit passes through the two-compartment differential cell (C) and then is focused by a fixed projector lens (P) and a movable microscope

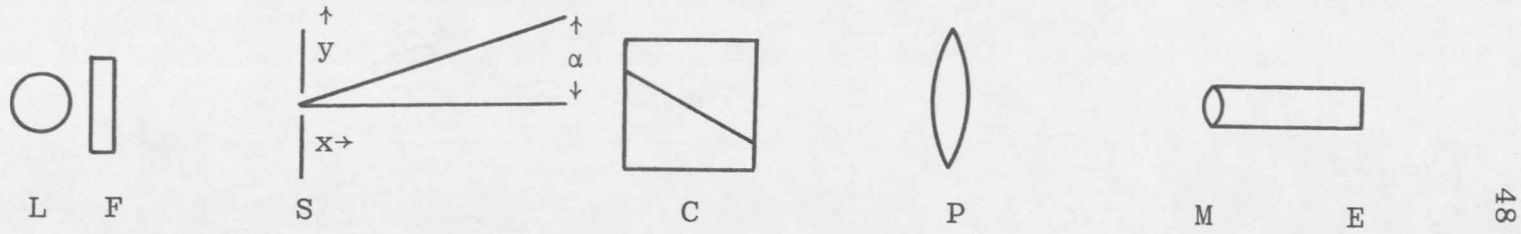

L = Mercury vapor lamp
F = Monochromatic filter
S = Slit
C = Two compartment cell
P = Projector lens
M = Microscope objective
E = Eyepiece scale (fixed to M)

Fig. 5.--Optical System of Brice-Phoenix Refractometer--Top View

objective (M). Moving the microscope assembly along the axis of the instrument allows a slit image to be focused on a 10 mm eyepiece scale (E) with a movable crosshair whose position can be read to 0.001 mm. The differential cell is mounted on a holder which can be rotated 180°.

The instrument is used to find refractive index differences between solutions and solvent by correlating the refractive index difference Δn with an instrument deflection Δd. With solvent in both compartments of the cell, a slit image is produced near the center of the eyepiece scale (undeflected image). When in one of the cell compartments solvent is replaced by the solution to be measured, a deflected image is produced to one side of the first position. When the cell is rotated 180° (i.e. when solvent and solution are interchanged) an image appears on the other side of the undeflected image position. The difference between the positions of these two deflected images, as observed on the eyepiece scale, is Δd. A relationship between Δd and Δn is then required.

Brice and Halwer, the refractometer designers, make the following statement in their discussion of the instrument:

> It will be shown that the difference in refractive index between solution and solvent is strictly proportional to Δd:

$$\Delta n = k\Delta d,$$

and that k can be evaluated either geometrically or by means of solutions of known refractive index. (39)

The particular instrument used in this laboratory has always been calibrated in the latter fashion and it has been found that the relationship of Δn to Δd is better represented by

$$\Delta n = k\Delta d + \ell(\Delta d)^2$$

than by the strict proportionality claimed by Brice and Halwer. When the instrument was calibrated with NaCl solutions for the work described in Part I the ratio $\Delta n/\Delta d$ showed a definite decrease in value with increasing Δn (Figure 6). The effect is not large--the drop is only about 1%--but it is measurable and is in contradiction to the assertion of Brice and Halwer.

It is not difficult to see in general why $\Delta n/\Delta d$ might not be constant. The procedure for obtaining Δd adds together deflections acquired in two very different optical situations. The refractometer cell is not symmetric across the optical axis of the instrument, and with solvent and solution in the two compartments a 180° rotation of the cell should not be expected to give equivalent deflections. Adding together nonequivalent deflections for a series of Δn values might then account for variations in $\Delta n/\Delta d$. The fact that the microscope assembly must be moved to bring the new

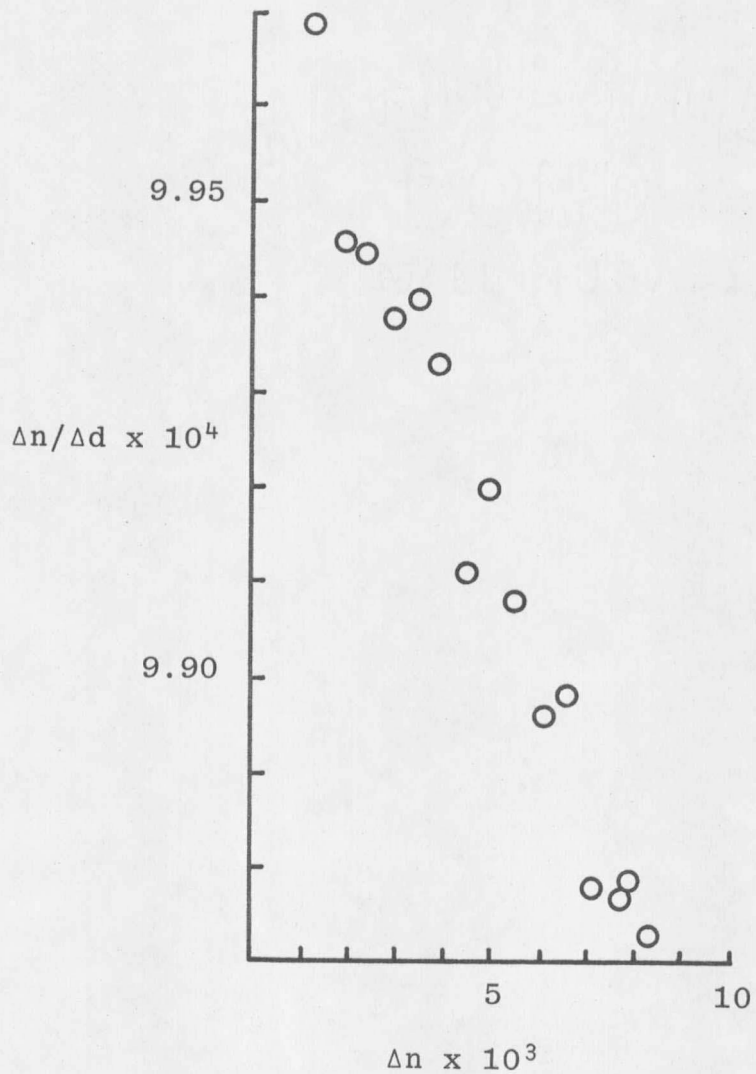

Fig. 6.--Data From Refractometer Calibration With NaCl

image into focus after rotation of the cell is experimental evidence for the nonequivalence. This effect is particularly noticeable with solutions showing large deflections.

Brice and Halwer developed an expression for calculating the presumed constant k in their relationship for $\Delta n/\Delta d$. Their characterization of the optical properties of the system is based upon tracing rays through the differential cell. Several approximations are made including the neglect of small terms and differences, and the neglect of the cell partition thickness. One of the factors that is used in their equations is the magnification that is achieved by the instrument from the slit to the eyepiece image. The magnification is a quantity which the authors have determined empirically for individual instruments. In the course of their development, expressions are obtained for locating the virtual slit image formed by the light rays which leave the cell after several refractions. According to Brice and Halwer the magnitude of the lateral displacement from the optical axis of the virtual slit image (SH) is given by

$$SH = (d_0 - d_2)/m$$

where

d_0 = scale reading with solvent in both compartments

d_2 = scale reading with solution in one compartment

m = magnification

The longitudinal position of the virtual slit image is calculated by tracing a slightly divergent ray from the slit through the cell and extrapolating the emergent ray back to its intersection with the optical axis. The assumptions are made that the cell partition can be ignored and that the other portions of the cell (solvent, solution, windows) can be considered as plane parallel plates. The equation obtained for the longitudinal distance (OS) of the virtual image from the slit is

$$OS = (b/2)(n_o-1)/n_o + (b/2)(n-1)/n + 2t(n_w-1)/n_w$$

where

b = distance between cell windows

t = thickness of cell windows

n_w = refractive index of glass

n_o = refractive index of solvent

n = refractive index of solution

The same equation is obtained by this method regardless of the relative positions of solvent and solution in the cell. In other words, this oversimplified model of the cell has removed any nonequivalence there might be in the longitudinal position of the virtual slit image before and after rotation of the cell. That there is an actual difference in these

images is subsequently acknowledged by the authors in connection with determining magnifications. They state that refocusing of the microscope is required when the cell is rotated and that this results in slightly different magnifications for the two positions. Their empirical data lead them to state that the average of these two magnifications is experimentally equal to the magnification obtained with solvent in both cell compartments. This approximation holds quite well for their data, but represents another instance in which the basic asymmetry of the optical system is being suppressed.

The expression for k which is ultimately derived by Brice and Halwer is

$$k = (\cot i)/2m_o(a + b/2n_o + t/n_w)$$

where

i = acute angle between partition and cell wall

m_o = magnification with solvent in both compartments

a = distance from slit to cell window

Since calibration experiments on the instrument in this laboratory yielded results different from those predicted by the designers ($\Delta n/\Delta d$ decreased with increasing n instead of remaining constant), and since there was reason to question the validity of the approximations in the

derivation of the equation for k, it was decided to test the conclusions of Brice and Halwer theoretically. This was done by constructing a computer program that would simulate the performance of a real refractometer. This program explicitly calculates, for a series of refractive indices, the positions of virtual slit image points and the positions of the focused real images both before and after rotation of the refractometer cell. Values of $\Delta n/\Delta d$ are also calculated for the refractive index series, and the magnification for each cell position and pair of refractive indices being compared can be determined from the calculated image coordinates. No approximations are introduced into the calculations. The program allows changes to be made in the various refractometer dimensions and parameters and also permits calculations to be made for two types of cell misalignment which might easily be found in a real instrument. The effect on image position can be determined for cases in which the cell center is not located on the rotational axis of the cell holder, when the entry face of the cell is not horizontally perpendicular to the optical axis, or for both situations combined. The computer program is presented in Appendix A.

EXPERIMENTAL

The experimental work of this part consisted of developing and using a computer program that would simulate the behavior of a real Brice-Phoenix refractometer. The calculations were based on straightforward trigonometry, analytical geometry, Snell's Law and the simple lens equations without simplifying assumptions about the cell geometry. Results are given to five significant figures. Variables and parameters in the calculations were declared as double precision. An inadvertent omission to do this with some of the quantities in one edition of the program showed small differences in results compared to the same calculations with double precision throughout.

The program establishes an x,y coordinate system at the center of the slit position. The directions of positive x and y are indicated in Figure 5. Two rays symmetrically divergent from the x axis at angles plus and minus alpha are traced from an image point on the y axis through the cell. The assumption is made initially that there is solution in the cell compartment nearer the source, and solvent in the other compartment. Coordinates of the exit points and the slopes of the two emergent rays are then used to calculate

the point from which these emergent beams appear to originate, i.e., the virtual image of the original point. This calculation can be made for points on the y axis other than $y = 0$, so it is possible to construct the appearance of an image of finite width after refraction through the cell. This allows a theoretical determination of the magnification of the simulated instrument. When the virtual image position has been calculated it is used as a real source for the fixed projector lens and the movable objective. The coordinates are then calculated for a real image produced at the focal plane of the objective by adjusting the position of this lens. At this point, the program exchanges refractive indices in the cell compartments and repeats the calculations. This gives the results of a 180° rotation of the cell. Each pair of calculations is performed for eleven values of solution refractive index. Assuming that the first of the eleven values is the refractive index of solvent, the program also calculates a series of $\Delta n/\Delta d$ values for the other ten refractive indices.

Each series of calculations requires values for solvent refractive index, the angle alpha, and the position of the source image point on the y axis, in addition to the eleven refractive indices for solution. In general the

solvent refractive index was chosen as 1.3400 (water at 25 C for 435.8 nm light). The solution values were 1.3400 (solvent in both compartments) up to 1.3500 in steps of 0.0010. This gave a reange of 0.01 refractive index units, which corresponds to the maximum range of the real refractometer.

Since the differential cell is not actually a lens, the coordinates of the virtual images show a small dependence on the value of alpha. This variation with angle becomes insignificant if alpha is chosen small enough, and for this reason an alpha value of 1×10^{-5} radian was used. This amounts to putting a second slit in front of the cell to produce very sharp images.

Focal lengths and cell dimensions for the computer model were taken from the instrument description by Brice and Halwer (39). Other dimensions were made to correspond with those of the instrument used in the light scattering studies of Part I.

When the program was modified to calculate for a cell displaced from the center of rotation and turned out of strict alignment, a slit image point was transferred to a new coordinate system. This system is located on a line perpendicular to the entry face of the cell and passing

through the cell center. When the slit image point is located in these new coordinates the calculation of the virtual image is carried out as in the original program. The location of the virtual image point is transformed back to the original coordinate system, and the focused real image is then found exactly as before. The 180^{o} cell rotation is accomplished by adjusting the x and y coordinates of the cell center in addition to exchanging the refractive indices in the two cell compartments.

DISCUSSION

The first result apparent from the computer calculations is that an experiment performed with a perfectly aligned and constructed instrument should show an increase in $\Delta n/\Delta d$ when it is plotted against Δn, rather than the decrease obtained in calibration of the instrument in this laboratory or the constant value predicted by Brice and Halwer. Figure 7 shows $\Delta n/\Delta d$ vs. Δn, and also shows the k value calculated for the simulated instrument from the equation of Brice and Halwer. The overall change in $\Delta n/\Delta d$ is small, being a rise of only about 0.4% in a 0.01 refractive index range corresponding to the maximum range of the actual instrument. The way in which the asymmetry of the instrument creates this result can be seen in Figure 8. For convenience in making comparisons $\Delta d/\Delta n$ rather than $\Delta n/\Delta d$ is plotted vs. Δn. Curve A shows the curve that is obtained if calculations are made without rotating the cell, and with solution in the compartment closer to the slit. Curve B is obtained for the series of calculations in which solvent is in the first compartment. It is apparent that the departures of $\Delta d/\Delta n$ from a constant value in the two curves are not symmetric and will not cancel out. The determination of

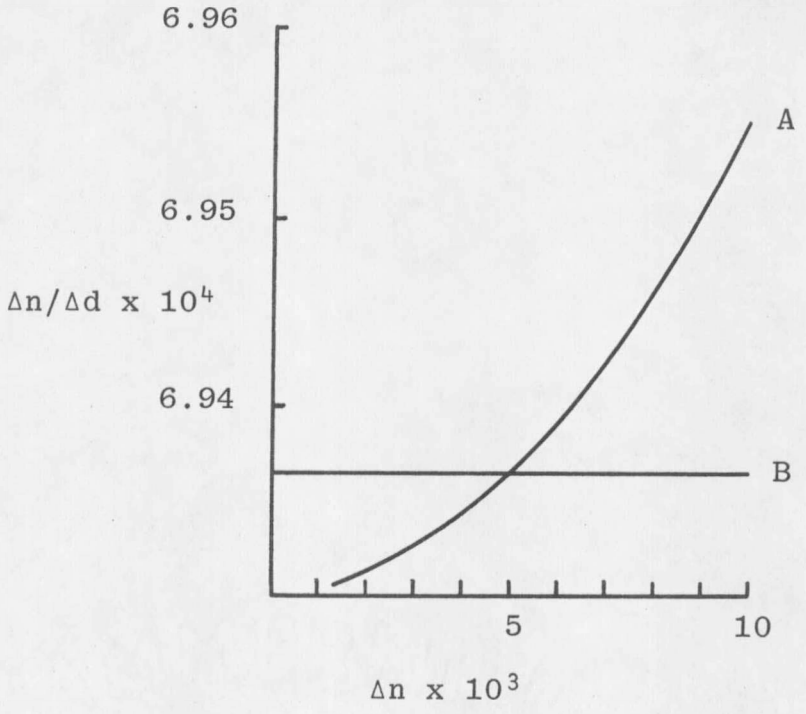

A = Δn/Δd from computer experiment

B = corresponding Δn/Δd by method of Brice and Halwer

Fig. 7.--Calculated Deflection Curves

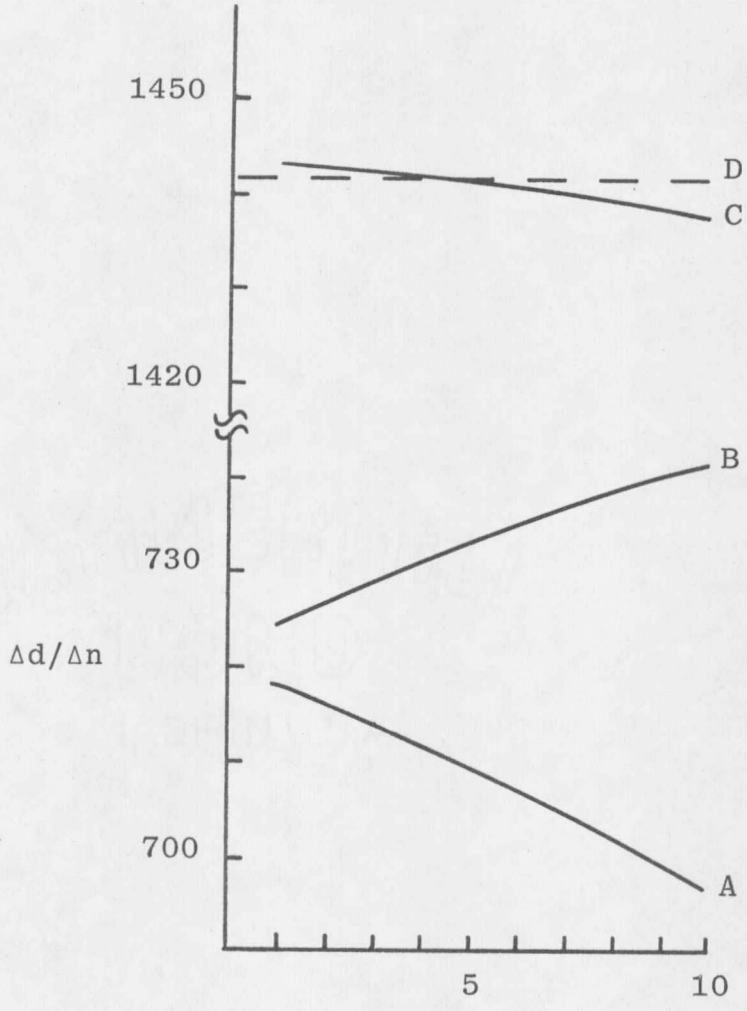

A = Single deflection curve, solution in first compartment

B = Single deflection curve, solvent in first compartment

C = Double deflection curve, = A + B

D = Δd/Δn by method of Brice and Halwer

Fig. 8.--Comparison of Deflection Curves

deflections by rotating the cell to get a larger net value of Δd, as in actual operation of the refractometer, produces a new curve (C) which is the sum of curves A and B.

By considering image points at x = 0, y = +1 and -1 mm, one can calculate the magnification of this instrument with the cell in each of the two different positions. This quantity is equal to the width of the focused image divided by the width of the slit (2mm). There is a small dependence of the magnification upon the refractive index of solution. This is illustrated in Table 6 which shows the magnification calculated for different solutions before (m) and after (m') rotation of the cell.

TABLE 6

MAGNIFICATIONS DETERMINED FOR SIMULATED INSTRUMENT

Solution Refractive Index	m	m'	Mean of m & m'
1.3400	2.0286	2.0286	2.0286 ($=m_o$)
1.3420	2.0283	2.0286	2.0284
1.3450	2.0285	2.0315	2.0300
1.3500	2.0312	2.0368	2.0338

m = magnification with solution toward slit
m'= magnification with solvent toward slit
solvent refractive index = 1.3400

The assumption of Brice and Halwer that m_o can be used as the average of m and m' is sound for solutions

differing only slightly in refractive index from solvent, but is slightly less accurate for higher concentrations.

It is particularly interesting to look at the positions of virtual slit images as calculated by the computer program and compared to the values predicted by the equations of Brice and Halwer. The computer program allows calculation of the image position of a slit of finite width, while the other approach only estimates the position of the image of the center point of the slit. As mentioned above, Brice and Halwer use separate approximations to find the lateral and longitudinal positions of the virtual slit image center point. The latter method is insensitive to the rotation of the cell. The comparison in approaches is illustrated in Figure 9 which is drawn to scale. Arrow A represents a 2mm wide slit bisected by the optical axis of the instrument. B is the computer calculated virtual image of this slit after tracing rays through the cell with solvent of refractive index 1.3400 in both compartments. With solution of refractive index 1.3420 in the compartment nearer the slit, the virtual image is C. Upon rotation of the cell the image becomes C'. The corresponding images for a solution with refractive index 1.3450 are D and D'. Point b is the center of the slit image for solvent vs. solvent

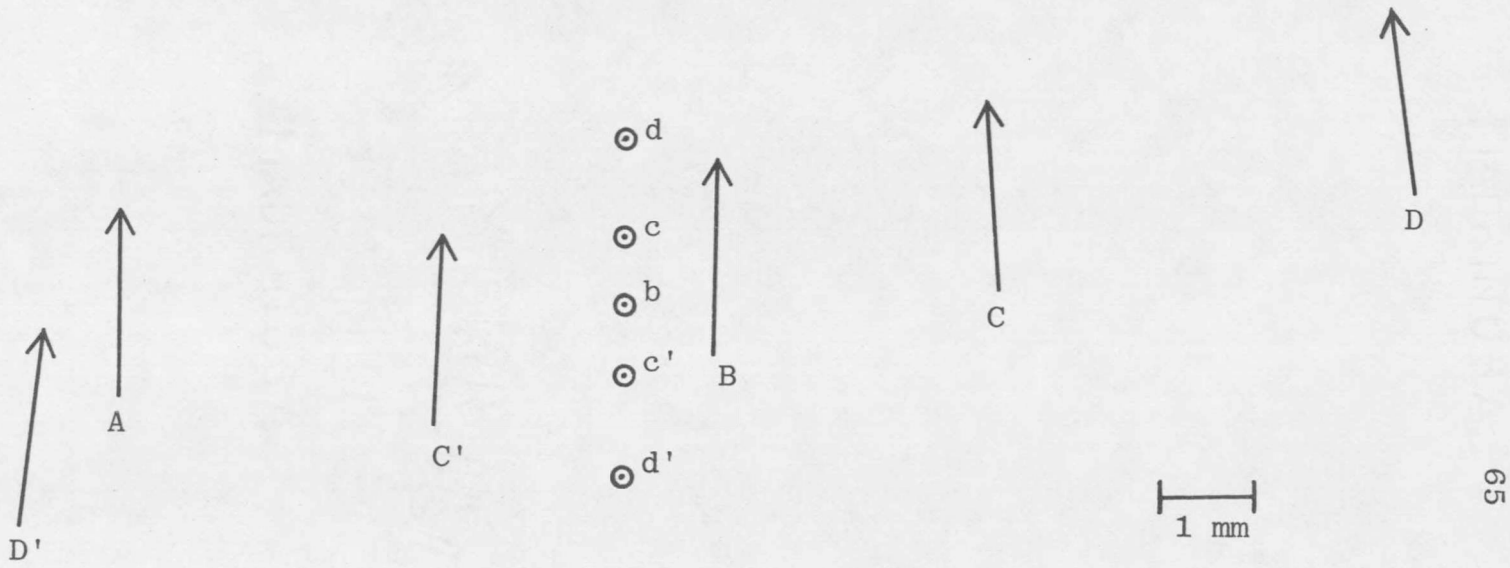

A = Image at slit
B = Virtual image with solvent (refractive index 1.340) in both compartments
C & C' = Virtual images with solution (1.342) in first and second compartments
D & D' = Virtual images with solution (1.345) in first and second compartments
b, c, c', d, d' = Midpoints of B, C, C', D, D' according to Brice and Halwer

Fig. 9.--Computer Calculated Slit Images Compared to Approximations of Brice and Halwer

calculated by the methods of Brice and halwer. Their approximations for the center points of C and C' are c and c' respectively. The same relationship holds for D and D' compared to d and d'. The values for the x coordinates of the points b, c & c', and d & d' are practically constant, being 5.3112, 5.3196 and 5.3320 mm respectively. These results demonstrate quite clearly the basic asymmetry in the operation of this type of refractometer and account for the necessity of refocusing the instrument after rotation of the cell.

The degree to which the approximations made by the designers are valid in characterizing their instrument was revealed by the computer model. There was still the question of what caused the instrument in this laboratory to give decreasing $\Delta n/\Delta d$ values for increasing Δn--a result at odds with the calculations for a perfect instrument. It was thought that the effect might be due to improper positioning and alignment of the cell. To test this possibility the computer program was modified to calculate on the basis of the cell center being displaced from the center of rotation either along the x axis, the y direction, or both. Allowance was also included for a cell that was rotated out of strict alignment by an angle beta (clockwise = positive).

Measurements made on the actual instrument used indicated that the cell was off center by about +0.3 mm in the x direction and about -0.2 mm in the y.

The calculated effects of separate x and y displacements of an otherwise aligned cell are shown in Figures 10 and 11. The curve for a perfectly aligned cell is included for comparison. The x and y displacements of 2.0 mm would be considered large for an actual instrument, but it is obvious that the character of the $\Delta n/\Delta d$ curve is not appreciably affected by even such large displacements. Smaller displacements than these produce curves that lie within the ranges that are plotted. The positions of these curves with respect to the vertical axis are sensitive to instrument dimensions. As an example, if the distance of the projector lens from the slit is changed from 442 mm to 433 mm, the initial point on the curve for complete cell alignment drops from a value of 7.173×10^{-4} (as in Figure 10) to 6.930×10^{-4} (as in Figure 7). Other points are similarly changed and the nature of the curve is not affected. Sets of curves presented for direct comparison are all based upon the same instrument constants, which closely approximate those of the actual refractometer.

The results of calculations made with different

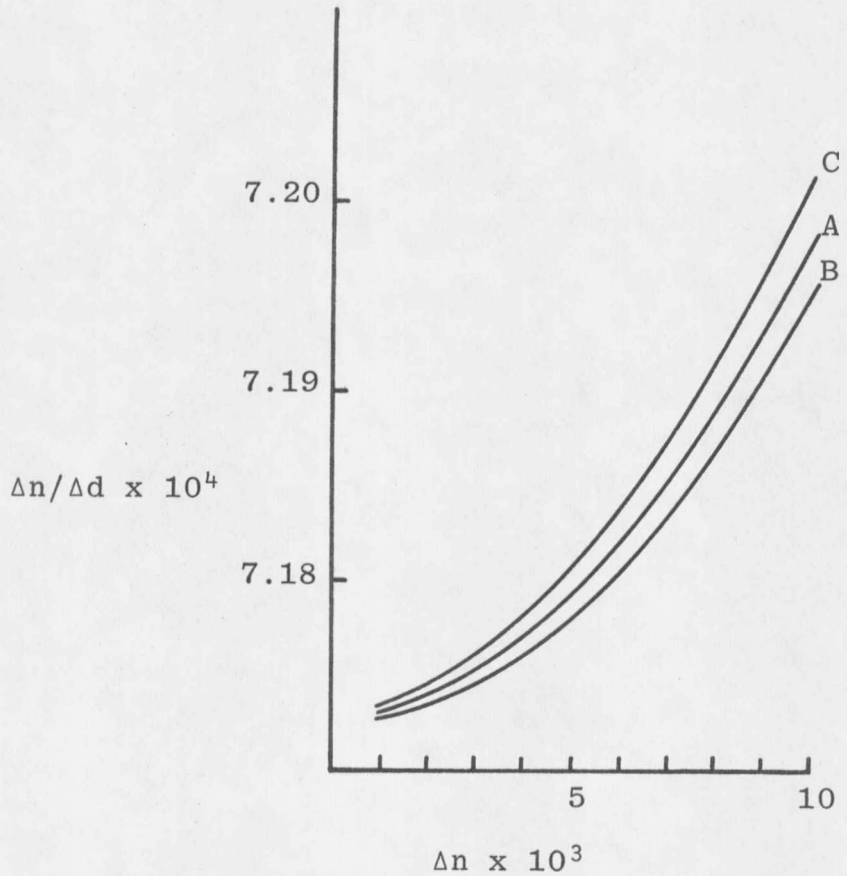

A: Displacement = 0

B: Displacement = +2 mm

C: Displacement = -2 mm

Fig. 10.--Effects of x Displacement of Cell

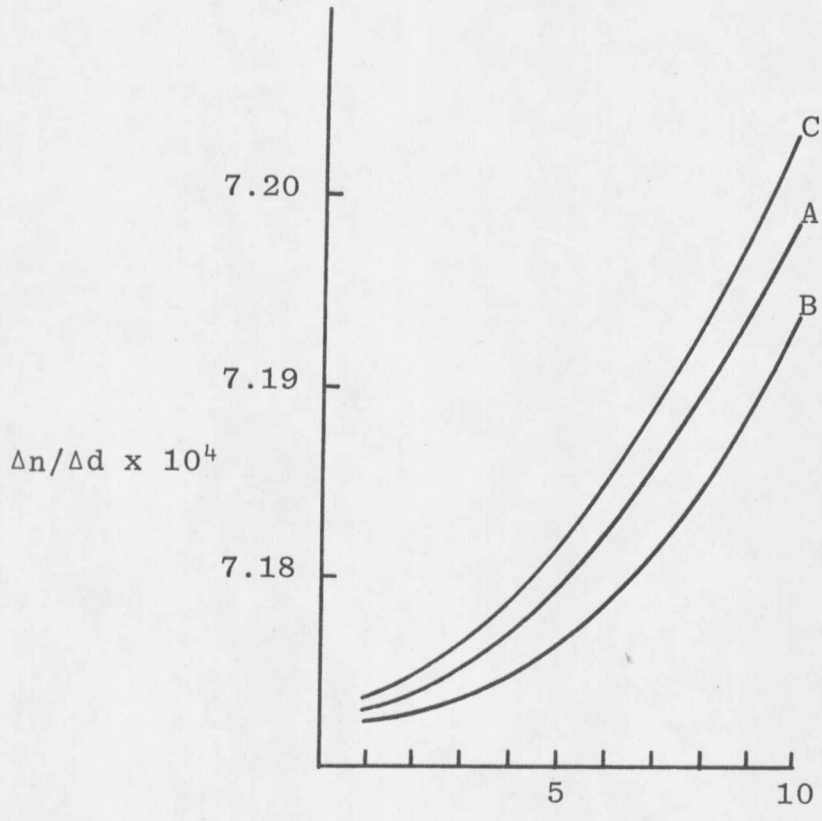

A: Displacement = 0

B: Displacement = +2 mm

C: Displacement = -2 mm

Fig. 11.--Effects of y Displacement of Cell

angular displacements are given in Figure 12. There are no significant changes in the nature of these curves if x and y displacements of the cell are also included. It is evident that a downward slope of the $\Delta n/\Delta d$ curve could be caused by a sufficiently large value of beta. This would require a beta value greater than 0.2 radian (about 11^{o}) and could hardly be overlooked when aligning the cell in an actual instrument.

Experiments with various instrument constants indicated that a downward slope of the curve could also be obtained if the focal length of the projector lens were larger than that given for the actual instrument. The increase in focal length required for this effect is on the order of twofold, and this does not seem a likely explanation for the behavior of the refractometer being studied.

In the Brice-Phoenix refractometer the cell rotation is performed by moving a handle attached to the cell holder. The handle is stopped at both ends of its swing by adjustable screws. A possible source of non-ideal behavior for this instrument would be a rotation angle of the cell which was different from 180^{o}. It is possible to calculate this effect from the results of the computer program by comparing the calculated deflections for a series of solutions with

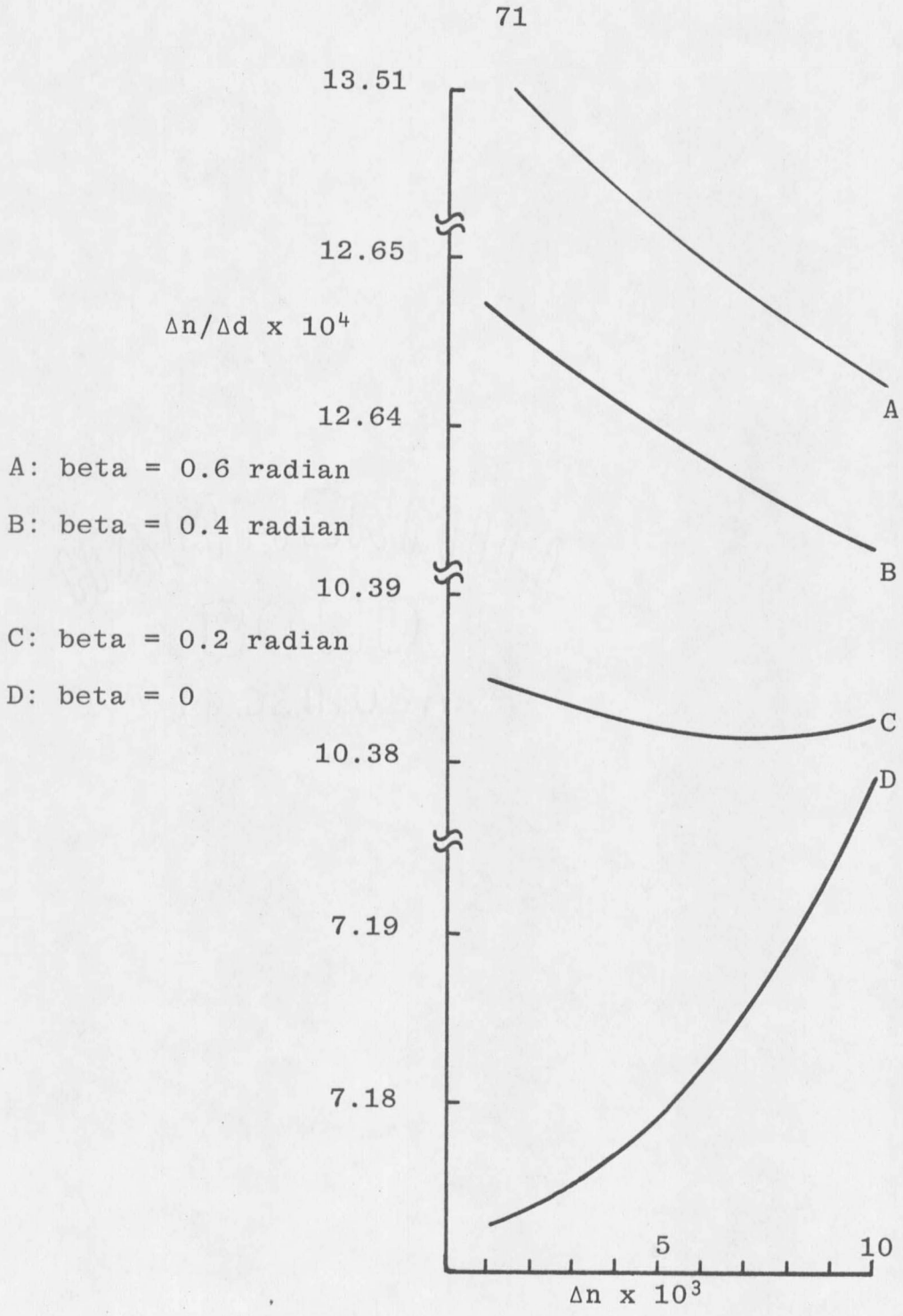

Fig. 12.--Effects of Beta

different values of beta for the two cell positions. This procedure shows that a negative slope for the curve can result from a rotation angle greater than 180^{o}. In Figure 13 curves are plotted for rotations of 180^{o} plus gamma for various gamma values. The positions of these curves with respect to the vertical scale depend upon the symmetry of the rotation. If the center of the rotation angle is toward the light source the curve will appear lower on the scale than if the center is toward the eyepiece. No appreciable difference is made when the center of the cell is displaced from the center of rotation. In figure 14 curves are plotted for several values of gamma of the order of 1×10^{-3} radian (0.06 degree). These curves represent rotation angles of different symmetries. This figure also shows the experimental points of Figure 6 artificially displaced downward by 2.9×10^{-4} units in order to fall in the same vertical range as the calculated curves. From this it is seen that small values of gamma could produce an effect of the magnitude detected experimentally. Unfortunately, the change to positive slope predicted by some of the calculations comes near the experimental limit of the refractometer, and this means of testing the explanation was not available without altering the instrument. This was not done in order that

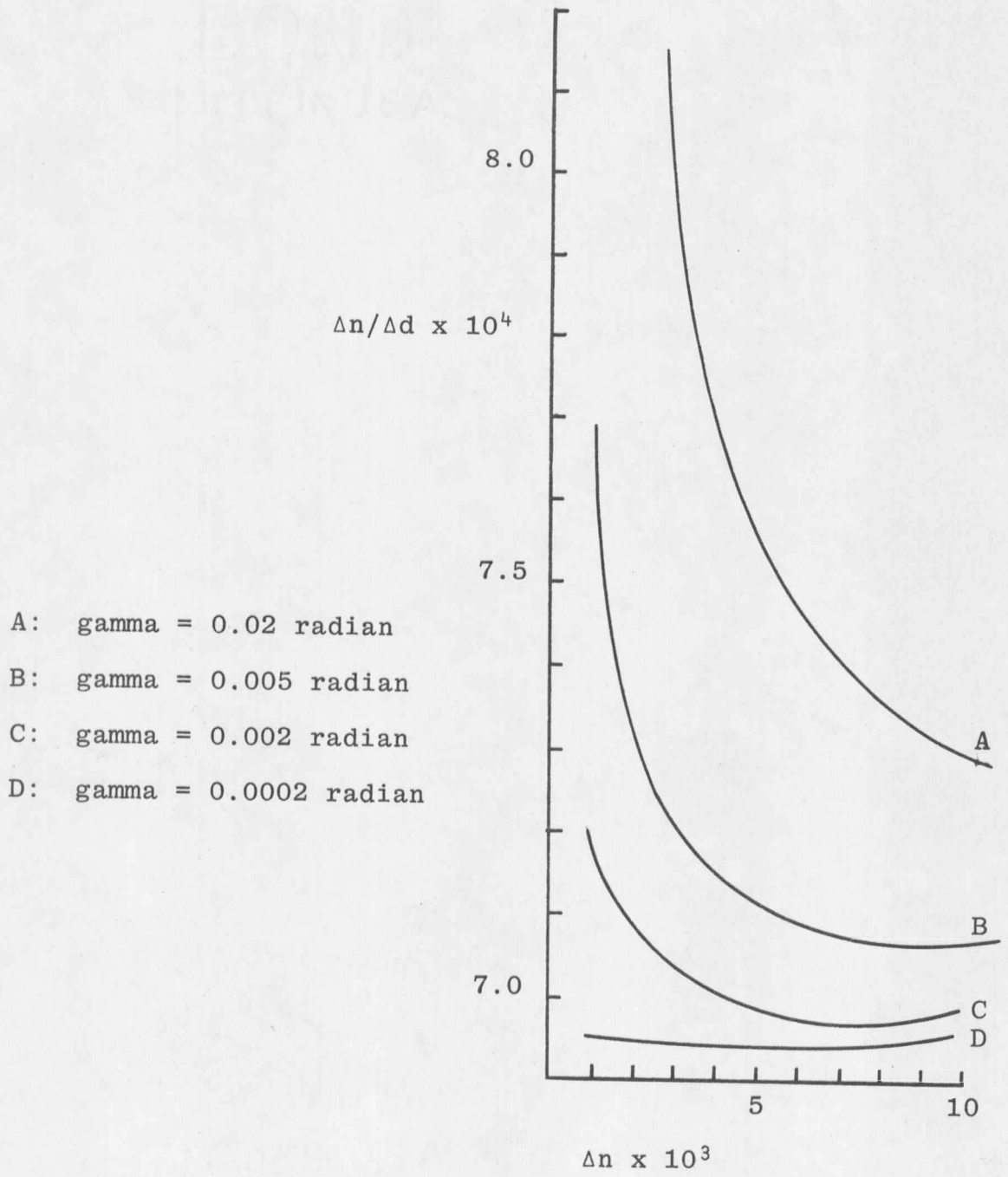

A: gamma = 0.02 radian

B: gamma = 0.005 radian

C: gamma = 0.002 radian

D: gamma = 0.0002 radian

Fig. 13.--Effects of Gamma (Small Scale)

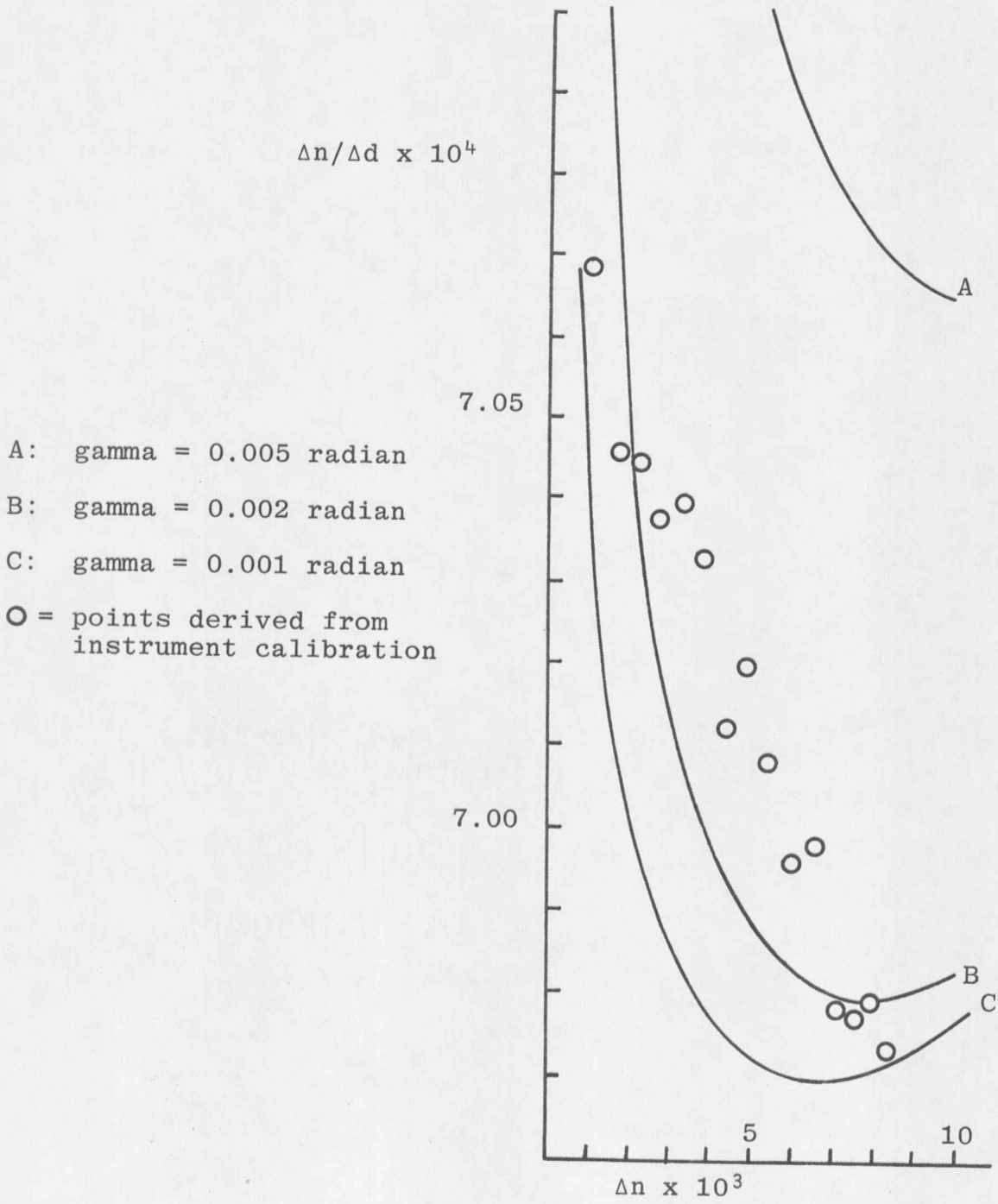

Fig. 14.--Effects of Gamma (Large Scale)

the instrument calibration be preserved.

While there is no assurance that a greater than 180° rotation is the reason for the non-ideality of the instrument in this laboratory, it is clear from this investigation that some small errors in alignment could account for the magnitude and kind of the effect detected. Other possible significant contributions to non-ideal behavior might arise from lenses and/or eyepiece scale not being perpendicular to the optical axis, from unparallel windows in the refractometer cell, or from misalignment of cell, optical axis, and the rotational axis of the cell holder.

It is concluded that in theory the highest possible accuracy cannot be obtained from the Brice-Phoenix refractometer by relying upon the approximate conclusions of Brice and Halwer. Although departure of their results from ideal behavior is not great, especially if only the lower half of the instrument range is used, the actual character of a particular instrument depends upon details of construction and alignment. In view of this conclusion, accurate calibration of this instrument from its geometry appears to be impractical for precise work. Calibration should be done empirically, and a proportional relationship between Δn and Δd should not be relied upon.

SUMMARY

Since there were detectable differences between experimental results obtained in this laboratory and the designer's description of performance for the Brice-Phoenix differential refractometer, the ideal performance of this type of instrument was determined by a computer program. This performance turned out to be different not only from the predictions of the designers (Brice and Halwer), but from the experimental results as well. The difference in performance between the ideal instrument and the assertions of Brice and Halwer is due to their neglect of the basic asymmetry of the refractometer. Due to a near averaging-out of the assymetry effects, Brice and Halwer's predictions are not greatly different from the ideal behavior.

Experiments were performed with the computer model in an effort to account for the behavior of the actual instrument used in light scattering studies. Linear or angular displacements of the refractometer cell from perfect alignment do not appear sufficient to explain the results obtained from the real instrument. A significant contribution to the observed non-ideal behavior could come from a slightly greater than 180^{o} rotation of the differential cell.

Although the possibility of calibrating the Brice-Phoenix refractometer from its geometry is claimed by the designers, this is not reliable for maximum performance of the instrument.

PART III

Surfactant Adsorption on Glass

INTRODUCTION

It is extremely important in light scattering work that solutions be free of dust particles which could scatter enough light to obscure the effects being studied. For this reason solutions prepared for scattering studies are usually filtered through an ultrafine fritted glass filter into the scattering cell. This procedure effectively removes dust particles, but in the event of surfactant adsorption on the filter the concentration of surfactant could be reduced significantly, especially when solutions of low concentration were being used. Adsorption of cationic surfactants on glass should be expected, since glass surfaces that have been treated with these surfactants are not uniformly wet by water. The adsorption of surfactant and concomitant reduction of its concentration in solution appears to be the likely explanation of some apparently anomalous light scattering data acquired in a study of cetylpyridinium chloride (5).

The typical plot of scattered light intensity vs. concentration for a series of solutions of a surfactant has a virtually horizontal, nearly zero, section at low concentrations. In some small concentration region, the critical

micelle "concentration" (CMC), the slope increases sharply upward. In the study of cetylpyridinium chloride (CPC) in 0.525 molar NaCl there were two breaks in the scattering curve obtained for the range 0 to 2 x 10^{-4} molar CPC (Figure 15).

These results can be accounted for if there were appreciable adsorption of CPC on the glass filter. It is assumed that the CMC of this compound would be found by extrapolating the upper linear portion of the curve back to the nearly horizontal section of the light scattering curve. The experimental points plotted beneath this extrapolation (and before it) would actually correspond to lower concentrations than indicated because of adsorption in the filter of a relatively high fraction of the CPC in the first few (most dilute) solutions. Upon saturation of the filter with CPC, the upper linear section would be obtained. If adsorption did not occur there would be only one break in the curve at the point where the extrapolated segment meets the horizontal part of the curve. To explore the feasibility of this argument a study was done to see if, in fact, CPC was adsorbed on fritted glass to a significant extent (40).

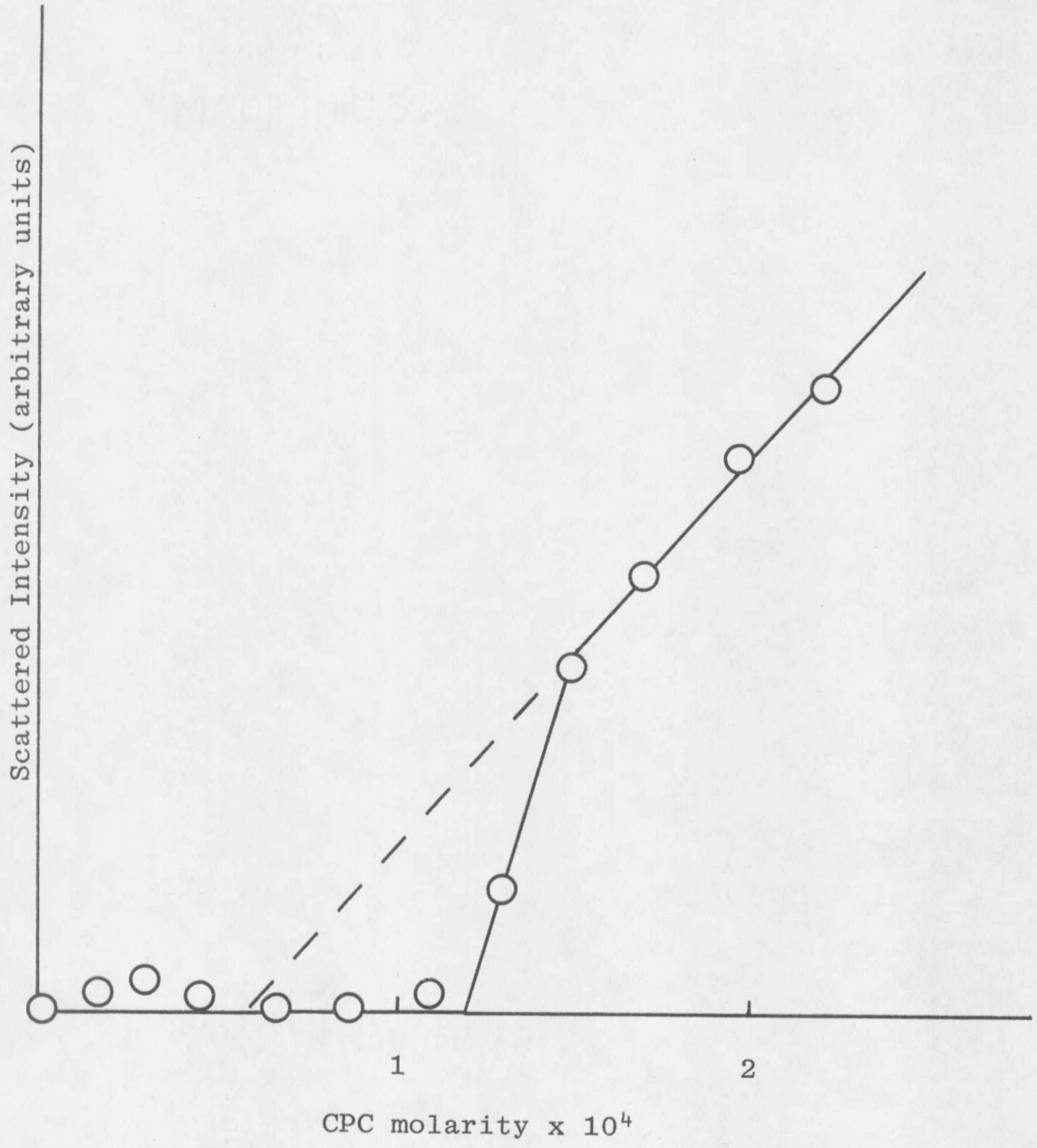

Fig. 15.--Light Scattering by Cetylpyridinium Chloride (5)

EXPERIMENTAL

A series of solutions of 9.3×10^{-5} molar CPC was prepared with NaCl concentrations ranging from 0.00 to 0.50 molar. Each solution was filtered through an ultrafine fritted Pyrex glass funnel. A sequence of from 17 to 34 small filtrate samples was collected for each solution. The amount of CPC present in these samples was determined by spectrophotometric analysis at 250 nm in a Beckman Model DU. Before each run the funnel was cleaned with hot concentrated sulfuric, nitric, and hydrochloric acids and rinsed with hot distilled water until the filtrate did not affect blue litmus. Analysis was also performed upon unfiltered samples of the CPC-NaCl solutions.

DISCUSSION

Measurements on unfiltered solutions showed that while NaCl has only a slight effect on the absorbance of water, it can, within limits, appreciably affect the absorbance of CPC solutions. There appears to be little effect from NaCl in concentrations greater than 0.25 molar (Table 7).

TABLE 7

ABSORBANCES OF 9.3×10^{-5} M CPC IN NaCl SOLUTIONS

M NaCl	Absorbance
0.00	0.37
0.01	0.38
0.10	0.40
0.25	0.42
0.50	0.42

When measurements were made on a series of filtered solutions, it was found in each case that the absorbances of the first few samples collected were very low, indicating considerable adsorption of CPC on the filter. With solutions low in NaCl (0.00, 0.01 molar) absorbance was much higher after the first two or three samples and absorbance values leveled off after the fifteenth of sixteenth samples. With higher concentrations of NaCl (0.10, 0.25, 0.50 molar) there was only a small increase in absorbance after the first few

samples and practically no further rise until after the twenty-fourth or twenty-fifth samples. After this there was a sharp rise in absorbance and a quick leveling off (Figure 16). For the range of samples between the initial few and those indicating near saturation of the filter, measured absorbances showed an inverse relationship to the concentration of NaCl. Within this range, the higher the NaCl concentration the lower the absorbance. It is apparent from this that the amount of CPC adsorbed is greatly dependent upon the concentration of NaCl. It is known (9, 10) that aggregation of surfactant monomers is enhanced by the presence of electrolytes. This suggests that the increased adsorption of CPC with NaCl concentration may be due to electrolyte promoted aggregation of monomers in solution with those adsorbed on the filter surface.

To avoid adsorption effects it has been the practice in this laboratory to do light scattering on a series of samples by passing several portions of the most dilute solutions through the filter to achieve adsorption saturation. This is especially important if solutions of very low surfactant concentration are being used.

In the light scattering investigations reported in Part I, the compounds studied all had CMC's which were

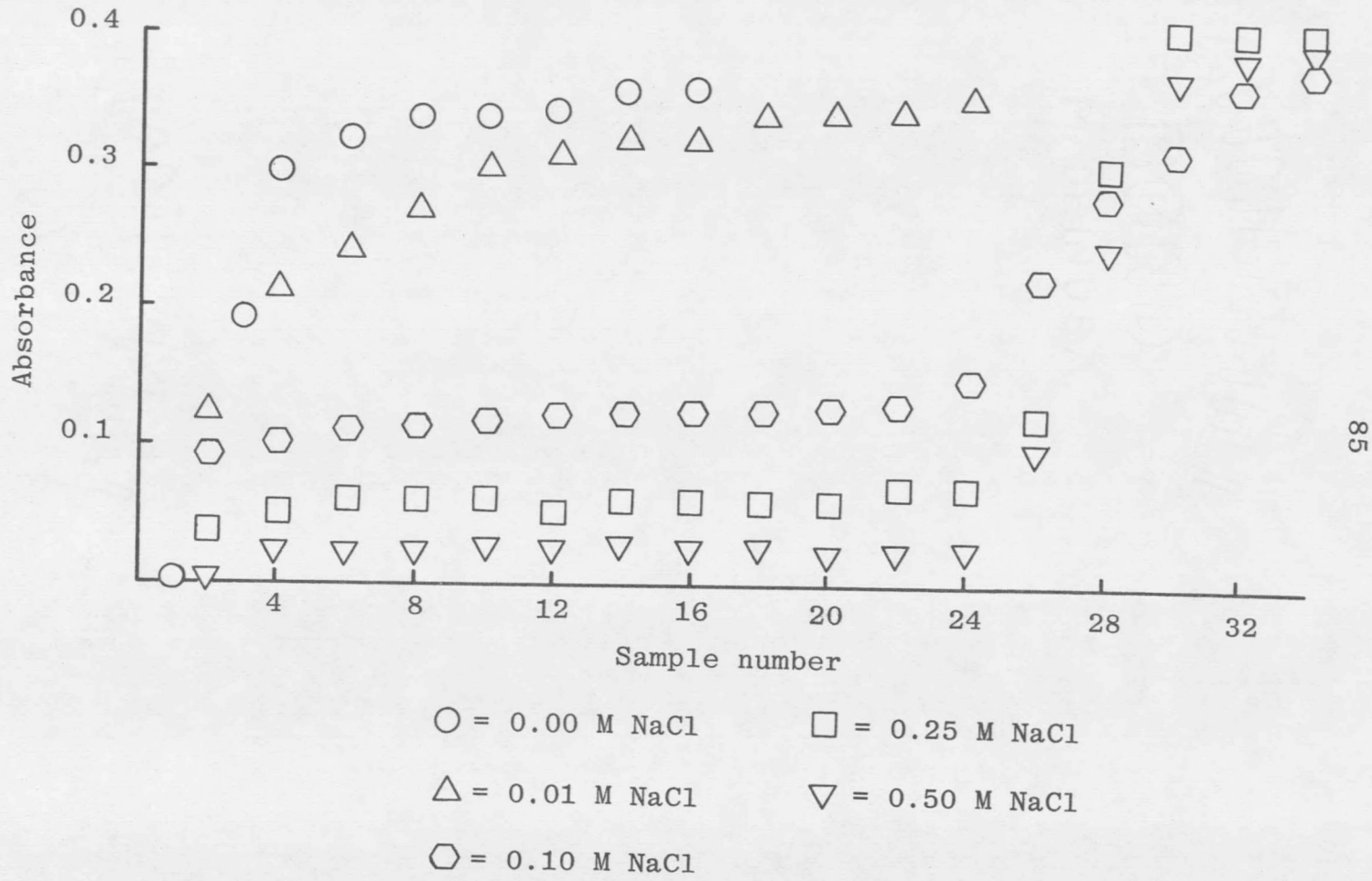

Fig. 16.--Absorbance of Filtered CPC (9.3×10^{-5} M) in NaCl at 260 nm

approximately 200 to 300 times greater than that for CPC. The light scattering curves for these materials showed no such apparent anomalies as those obtained in the CPC study and accounted for by adsorption of the surfactant. Nevertheless, it is probable that adsorption of these compounds did occur, but that working in a higher concentration range allowed saturation of the filter by passage of solutions well under the CMC. In one case, adsorption of the surfactant was evident. The compound decyl-4-cyanopyridinium bromide has an intense yellow color, unlike all the other surfactants used which are colorless. When a series of solutions of this compound was filtered, the filter acquired a yellow color which visibly increased in intensity up to about the CMC.

An attempt was made to determine with a precision pH meter the pH of various surfactant solutions studied in Part I. It was not possible to get reproducible and consistent results. Adsorption of surfactant on the membrane of the glass electrode may well have contributed to the erratic results obtained.

SUMMARY

Surfactant adsorption on glass can definitely occur, and an investigator performing light scattering work should be alert to the possible effects of this phenomenon on data from solutions of low concentration.

LIST OF REFERENCES

1. J. W. McBain, Trans. Faraday Soc., 9, 99 (1913).

2. D. Stigter, J. Colloid Interface Sci., 23, 379 (1967).

3. D. C. Poland and H. A. Scheraga, J. Phys. Chem., 69, 2431 (1965).

4. D. C. Poland and H. A. Scheraga, J. Colloid Interface Sci., 21, 273 (1966).

5. E. W. Anacker, J. Phys. Chem., 62, 41 (1958).

6. D. Stigter, J. Phys. Chem., 68, 3603 (1964).

7. H. V. Tartar, J. Phys. Chem., 59, 1195 (1955).

8. E. W. Anacker and H. M Ghose, J. Am. Chem. Soc., 90, 3161 (1968).

9. P. Debye, Ann. N. Y. Acad. Sci., 51, 575 (1947).

10. P. Debye and E. W. Anacker, J. Phys. and Colloid Chem., 55, 644 (1951).

11. P. Debye, J. Appl. Phys., 15, 338 (1944).

12. P. Debye, J. Phys. Chem., 51, 18 (1947).

13. A. Vrij, Thesis, University of Utrecht, 1959.

14. A. Vrij and J. Th. G. Overbeek, J. Colloid Sci., 17, 570 (1962).

15. E. F. Casassa and H. Eisenberg, J. Phys. Chem., 64, 753 (1960).

16. D. Stigter, J. Phys. Chem., 64, 842 (1960).

17. W. Prins and J. J. Hermans, Koninkl. Ned. Akad. Wetenschap. Proc., B59, 162 (1956).

18. K. J. Mysels, J. Colloid Sci., 10, 507 (1955).

19. L. H. Princen and K. J. Mysels, J. Colloid Sci., 12, 594 (1957).

20. K. J. Mysels and L. H. Princen, J. Phys. Chem., 63, 1696 (1959).

21. G. Scatchard and J. Bregman, J. Am. Chem. Soc., 81, 6095 (1959).

22. E. W. Anacker and A. E. Westwell, J. Phys. Chem., 68, 3490 (1964).

23. E. W. Anacker, Ph. D. Thesis, Cornell Univ., (1949).

24. E. W. Anacker and H. M. Ghose, J. Phys. Chem., 67, 1713 (1963).

25. M. L. Corrin and W. D. Harkins, J. Am. Chem. Soc., 69, 683 (1947).

26. R. D. Geer, E. H. Eylar and E. W. Anacker, J. Phys. Chem., 75, 369 (1971).

27. E. W. Anacker and R. D. Geer, J. Colloid Interface Sci., 35, 441 (1971).

28. P. T. Jacobs and E. W. Anacker, J. Colloid Interface Sci., 44, 505 (1973).

29. A. Veis and C. W. Hoerr, J. Colloid Sci., 15, 427 (1960).

30. R. A. Barnes, in Pyridine and its Derivatives (E. Klingsberg, ed.), Part I, Interscience, New York, 1960, p. 35.

31. Ibid p. 30.

32. J. A. Stead and H. Taylor, J. Colloid Interface Sci., 30, 482 (1969).

33. A. Kruis, Ziet. Phys. Chem., 34B, 13 (1936).

34. P. T. Jacobs, R. D. Geer and E. W. Anacker, J. Colloid Interface Sci., 39, 611 (1972).

35. L. E. Tenebaum, in Pyridine and its Derivatives (E. Klingsberg, ed.), Part II, Interscience, New York, 1961, p. 203.

36. P. T. Jacobs and E. W. Anacker, J. Colloid Interface Sci., 43, 105 (1973).

37. A. Streitwieser Jr., Molecular Orbital Theory for Organic Chemists, John Wiley and Sons, Inc., New York, 1961, p. 135.

38. S. P. McGlynn, L. G. Vanquickenborne, M. Kinoshita and D. G. Carroll, Introduction to Applied Quantum Chemistry, Holt, Rhinehart and Winston, Inc., New York, 1972, p.87.

39. B. A. Brice and M. Halwer, J. Opt. Soc. Am., 41, 1033 (1951).

40. A. E. Westwell and E. W. Anacker, J. Phys. Chem., 63, 1022 (1959).

41. H. S. Frank and M. W. Evans, J. Chem. Phys., 13, 507 (1945).

42. P. Mukerjee, Advan. Colloid Interface Sci., 1, 241 (1967).

APPENDICES

APPENDIX A

Computer Program for Simulation of Refractometer

```
C THIS PROGRAM SIMULATES PERFORMANCE OF BRICE-PHOENIX DIFFERENTIAL
C  REFRACTOMETER. REFERENCE: BRICE & HALWER, J. OPT. SOC. AM.,41, 1033
C  (1951).  DIVERGENT LIGHT RAYS ARE TRACED FROM A POINT SOURCE
C  THROUGH THE DIFFERENTIAL CELL AND THE SYSTEM OF LENSES. POSITIONS
C  ARE COMPUTED BEFORE AND AFTER CELL ROTATION FOR THE VIRTUAL IMAGE
C  PRODUCED BY THE CELL AND FOR THE FOCUSED REAL IMAGE IN THE EYEPIECE
C  FIELD. CELL CAN BE OUT OF ALIGNMENT IN X-Y DIRECTIONS AND BY AN
C  ANGLE. OPTICAL AXIS IS X AXIS, Y AXIS PASSES THROUGH SOURCE.
C  CALCULATIONS ARE ALSO MADE FOR REFRACTIVE INDEX INCREMENT VERSUS
C  IMAGE DISPLACEMENT.
      DOUBLE PRECISION A,AA,AL,BETA,C,COSC,COSEP,COSTH,COTC,D,DD,DOI,DPR
     1O,E,ES,EX,F1,F2,KAY,N,P,RE,RS,RW,S,SINAL,SINC,SINEP,SINRH,SINSI,SI
     1NTH,SLOPE,SP,T,TANCEP,TANCTH,TANGA,TX,TXFI,TXP,TY,TYFI,TYP,TYS,W,W
     1Y,X,XFI,XFIP,XP,X2,X3,X4,X5,X6,Y,YFI,YFIP,YIE,YIS,YP,YPOINT,YS,Y1,
     1Y2,Y3,Y4,Y5,Y6,Y6P,SINB,COSB
      DIMENSION YS(20),EX(20),WY(20),BETA(20),RS(11),DD(11),N(11),KAY(11
     2),XP(20,11),YP(20,11),XFIP(20,11),YFIP(20,11),X(20,11),Y(20,11),
     2XFI(20,11),YFI(20,11)
C A NUMBER OF PARAMETERS ARE GIVEN BY DATA DECLARATION.  THESE ARE
C  DEFINED BELOW.  LINEAR DIMENSIONS ARE IN MILLIMETERS, ANGLES ARE
C  IN RADIANS.
C     A = DISTANCE FROM SOURCE TO ENTRY FACE OF PERFECTLY ALIGNED CELL
C     T = THICKNESS OF CELL WINDOWS
C     W = DISTANCE BETWEEN CELL WINDOWS
C     C = ACUTE ANGLE BETWEEN CELL WINDOW AND CELL PARTITION
C     P = THICKNESS OF CELL PARTITION
C     RW = REFRACTIVE INDEX OF GLASS USED IN CELL
C     RE = REFRACTIVE INDEX OF SOLVENT
C     RS = REFRACTIVE INDEX OF SOLUTION, 11 VALUES REQUIRED,FIRST = RE
C     F1 = FOCAL LENGTH OF PROJECTOR LENS
C     F2 = FOCAL LENGTH OF MICROSCOPE OBJECTIVE
C     DPRO = DISTANCE FROM SOURCE TO PROJECTOR LENS
C     DOI = DISTANCE BETWEEN OBJECTIVE LENS AND IMAGE FIELD
C     AL = ALPHA, ANGLE BETWEEN OPTICAL AXIS AND RAY BEING TRACED
      DATA A,T,W,C,P,RW/1.2240D 02,2.2000D 00,1.5000D 01,1.22173D 00,
```

```
     31.1200D 00,1.5200D 00/,
     3RE,(RS(M),M=1,11)/1.3400D 00,1.3400D 00,1.3410D 00,1.3420D 00,
     31.3430D 00,1.3440D 00,1.3450D 00,1.3460D 00,1.3470D 00,
     31.3480D 00,1.3490D 00,1.3500D 00/,
     3F1,F2,DPRO,DOI/1.6400D 02,4.0000D 01,4.3300D 02,1.7000D 02/,
     3AL/1.0000D-05/
  11 FORMAT(42H1VIRTUAL INTERSECTION OF EXIT RAYS FOR RE=,1PD11.4,8H  A
     4LPHA=,1PD11.4,5H  YS=,1PD11.4,33H  AND COORDINATES OF THEIR IMAGES
     4//20X,24HCELL DISPLACEMENTS:  EX=,1PD11.4,5H  WY=,1PD11.4,7H  BETA
     4=,1PD11.4//20X,2HRS,12X,1HX,11X,1HY,11X,3HXFI,9X,3HYFI,13X,2HXP,10
     4X,2HYP,10X,4HXFIP,8X,4HYFIP//11(17X,1PD10.4,1X,1P2D12.4,1X,1P2D12,
     44,3X,1P2D12.4,1X,1P2D12.4//)1H1,8X,1HN,14X,1HD,11X,8HKAY= N/D//
     410(1P3D15.4/))
  12 FORMAT(1PD11.4,1P3D12.4,I2)
     I=1
C READ DATA CARDS.  THESE CARDS CONTAIN THE QUANTITIES DEFINED BELOW.
C  LINEAR DIMENSIONS ARE IN MILLIMETERS, BETA IS IN RADIANS.
C     YS = DISTANCE OF SOURCE POINT FROM OPTICAL AXIS
C     EX = X-DISPLACEMENT OF CELL CENTER FROM CENTER OF ROTATION
C     WY = Y-DISPLACEMENT OF CELL CENTER FROM CENTER OF ROTATION
C     BETA = ANGULAR DISPLACEMENT OF CELL FROM OPTICAL AXIS, (CLOCKWISE
C            = POSITIVE).
C  ON DATA CARDS, YS IS RECORDED IN COLUMNS 1-11, EX IN 13-23, WY IN
C  25-35, BETA IN 37-47.  LAST DATA CARD USES SPACES 48 & 49 TO RECORD
C  THE NUMBER OF DATA CARDS (K).  LIMIT IS 20 CARDS.
  20 READ(105,12) YS(I),EX(I),WY(I),BETA(I),K
     I=I+1
C CHECK FOR END OF DATA DECK
     IF(K.EQ.0) GO TO 20
C DEFINE PARAMETERS BASED ON CELL CHARACTERISTICS
     ES= T+W/2.
     SINC=DSIN(C)
     COSC=DCOS(C)
     COTC=COSC/SINC
C START DO LOOP FOR SEQUENCE OF DATA CARDS
```

```
      DO 30 I=1,K
C  DEFINE PARAMETERS BASED ON ANGULAR CELL DISPLACEMENT
      SINB =DSIN(BETA(I))
      COSB=DCOS(BETA(I))
C  START DO LOOP FOR SERIES OF SOLUTION REFRACTIVE INDICES
      DO 28 M=1,11
      L=0
      J=0
C  PUT SOLUTION IN CELL COMPARTMENT NEAR SOURCE, SOLVENT IN OTHER SIDE
      D=RE
      E=RS(M)
C  PARAMETERS DEFINED FOR NEW COORDINATE SYSTEM WITH X AXIS THROUGH
C   CELL CENTER PERPENDICULAR TO CELL WINDOW,& Y AXIS THROUGH SOURCE
   21 AA=(A+EX(I)+ES)*COSB+(YS(I)-WY(I))*SINB-ES
      TYS=(YS(I)-WY(I))/COSB-((A+EX(I)-ES)*COSB+(YS(I)-WY(I))*SINB-2.*ES
     5)*(SINB/COSB)
      YIS=COTC*(AA+T+(W-P/COSC)/2.)
      YIE=YIS+P/SINC
      X2=AA+T
      X5=AA+T+W
C  COMPUTE X COORDINATE OF POINT WHERE TRACED RAY LEAVES CELL
      X6=AA+2.*T+W
C  ASSIGN ANGLE OF DIVERGENCE FOR FIRST RAY TO BE TRACED
      SINAL=DSIN(AL+BETA(I))
C  COMPUTE SLOPE OF RAY EMERGING FROM CELL (= S FOR FIRST RAY TRACED,
    = SP FOR SECOND RAY TRACED)
   22 SINRH=SINC*DSQRT(D**2-(SINC*DSQRT(E**2-SINAL**2)-COSC*SINAL)**2)-
     6 COSC*(SINC*DSQRT(E**2-SINAL**2)-COSC*SINAL)
      SLOPE=SINRH/DSQRT(1.-SINRH**2)
      IF (L.LT.1) GO TO 24
      SP= SLOPE
C  COMPUTE Y COORDINATE OF POINT WHERE TRACED RAY LEAVES CELL
C     = Y6 FOR FIRST RAY TRACED
C     = Y6P FOR SECOND RAY TRACED
   23 Y1= TYS+AA*SINAL/DSQRT(1.-SINAL**2)
```

```
      Y2=Y1+T*SINAL/DSQRT(RW**2-SINAL**2)
      TANGA=SINAL/DSQRT(E**2-SINAL**2)
      X3=(YIS-Y2+X2*TANGA)/(TANGA+COTC)
      Y3=YIS-X3*COTC
      SINEP=(SINC*DSQRT(E**2-SINAL**2)-COSC*SINAL)/RW
      COSEP=DSQRT(1.-SINEP**2)
      TANCEP=(SINC*COSEP-COSC*SINEP)/(COSC*COSEP+SINC*SINEP)
      X4=(YIE-Y3+X3*TANCEP)/(TANCEP+COTC)
      Y4=YIE-X4*COTC
      SINTH=RW/D*SINEP
      COSTH=DSQRT(1.-SINTH**2)
      TANCTH=(SINC*COSTH-COSC*SINTH)/(COSC*COSTH+SINC*SINTH)
      Y5=Y4+(X5-X4)*TANCTH
      SINSI=D/RW*(SINC*COSTH-COSC*SINTH)
      YPOINT=Y5+T*(SINSI/DSQRT(1.-SINSI**2))
      IF (L.GT.0) GO TO 25
      Y6=YPOINT
C  COMPUTE INTERSECTION (VIRTUAL IMAGE POINT) OF TWO TRACED RAYS
C   X & Y COORDINATES = TXP & TYP
      TXP= X6-(Y6-Y6P)/(S-SP)
      TYP= Y6-S*(Y6-Y6P)/(S-SP)
C  VIRTUAL IMAGE POINT TRANSFORMED TO ORIGINAL COORDINATE SYSTEM(TX&TY)
      TY=TYP*COSB+((A+EX(I)+ES)*COSB+(YS(I)-WY(I))*SINB-2.*ES-TXP)*SINB+
     7WY(I)
      TX=(TXP+(TY-YS(I))*SINB)/COSB
C  COMPUTE COORDINATES OF FOCUSED IMAGE IN EYEPIECE FIELD
C   BEFORE ROTATION VIRTUAL IMAGE COORDINATES ARE X & Y, FOCUSED IMAGE
C   COORDINATES ARE XFI & YFI.  AFTER CELL ROTATION COORDINATES ARE
C   XP, YP, & XFIP, YFIP
      TXFI=(F1*TX-DPRO*(DPRO-TX))/(F1+TX-DPRO)-DOI*F2/(F2-DOI)+DOI
      TYFI=TY*F1*(DOI-F2)/(F2*(DPRO-F1-TX))
      IF (J.LT.1) GO TO 26
      XP(I,M)=TX
      YP(I,M)=TY
      XFIP(I,M)=TXFI
```

```
      YFIP(I,M)=TYFI
      GO TO 27
   24 S=SLOPE
C  ASSIGN ANGLE OF DIVERGENCE FOR SECOND RAY TO BE TRACED
      SINAL=DSIN(BETA(I)-AL)
      L=1
      GO TO 22
   25 Y6P=YPOINT
C  REASSIGN ANGLE OF DIVERGENCE FOR FIRST RAY TO BE TRACED
      L=0
      SINAL=DSIN(AL+BETA(I))
      GO TO 23
   26 X(I,M)=TX
      Y(I,M)=TY
      XFI(I,M)=TXFI
      YFI)I,M)=TYFI
      J=1
C  CELL ROTATED BY EXCHANGING REFRACTIVE INDICES AND BY ADJUSTING X & Y
C   CELL DISPLACEMENTS
      D=RS(M)
      E=RE
      EX(I)=-EX(I)
      WY(I)=-WY(I)
      GO TO 21
   27 CONTINUE
C  RESTORE ORIGINAL X & Y CELL DISPLACEMENTS FOR CALCULATION WITH
C   NEXT REFRACTIVE INDEX
      EX(I)=-EX(I)
      WY(I)=-WY(I)
C  CALCULATIONS WILL REPEAT FOR NEXT SOLUTION REFRACTIVE INDEX
   28 CONTINUE
C  START DO LOOP FOR REFRACTIVE INDEX INCREMENT (N), FOCUSED IMAGE
C   DEFLECTION (D) AND THEIR RATIO: KAY =N/D
      DO 29 M=2,11
      DD(M)=YFI(I,M)-YFIP(I,M)
```

```
      N(M)=RS(M)-RS(1)
      KAY(M)=N(M)/DD(M)
C  CALCULATION OF KAY REPEATED FOR NEXT SOLUTION REFRACTIVE INDEX
   29 CONTINUE
C  RESULTS PRINTED FOR THE SEQUENCE OF 11 SOLUTION REFRACTIVE INDICES
C   SYMBOLS USED ARE DEFINED IN PREVIOUS COMMENTS
      WRITE(108,11) RE,AL,YS(I),EX(I),WY(I),BETA(I),(RS(M),X(I,M),Y(I,M
     8),XFI(I,M),YFI(I,M),XP(I,M),YPI,M),XFIP(I,M),YFIP(I,M),M=1,11),
     8(N(M),DD(M),KAY(M),,=2,11)
C  CALCULATIONS WILL REPEAT FOR NEXT DATA CARD IN SEQUENCE (MAXIMUM 20)
   30 CONTINUE
      END
```

APPENDIX B

Experimental Data for Determination of Aggregation Numbers

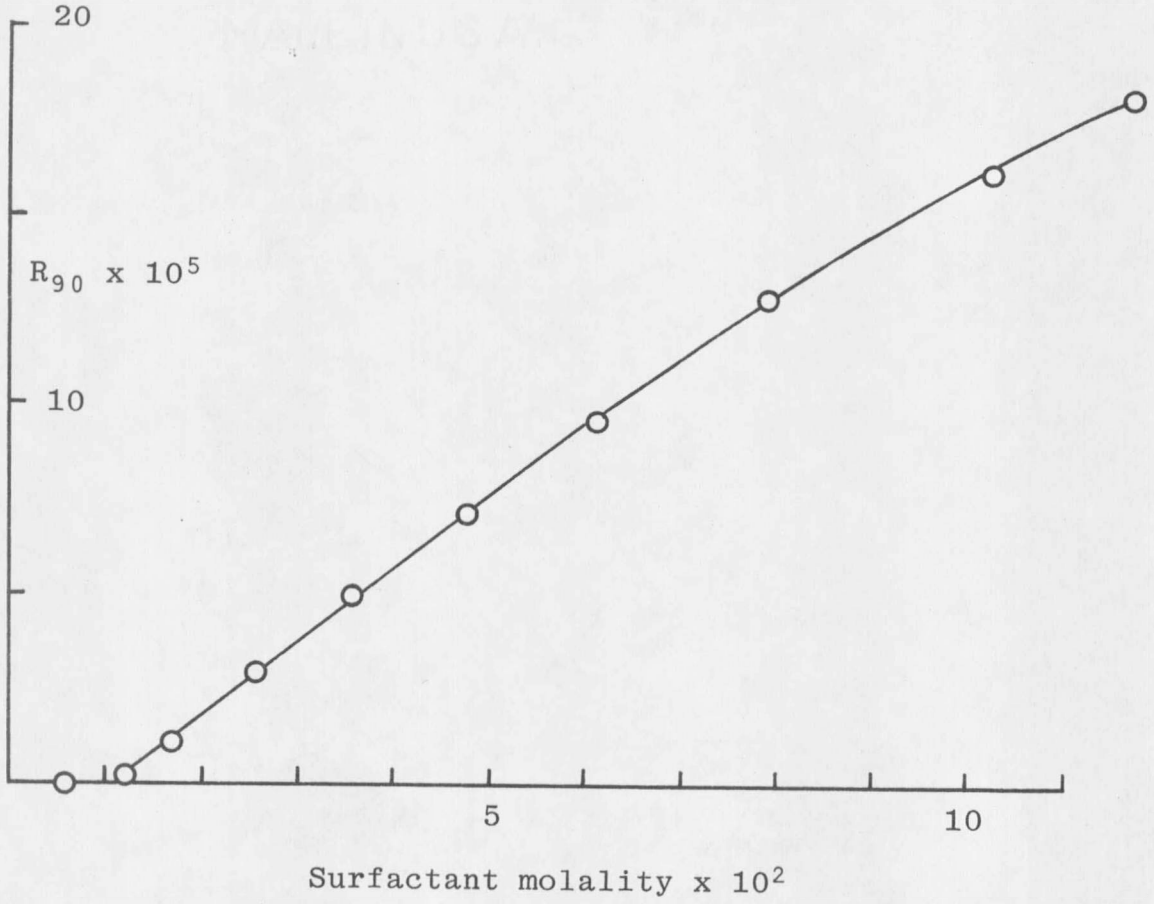

Fig. 17.--Light Scattering Data for DPB in 0.5 m NaBr, 25° C

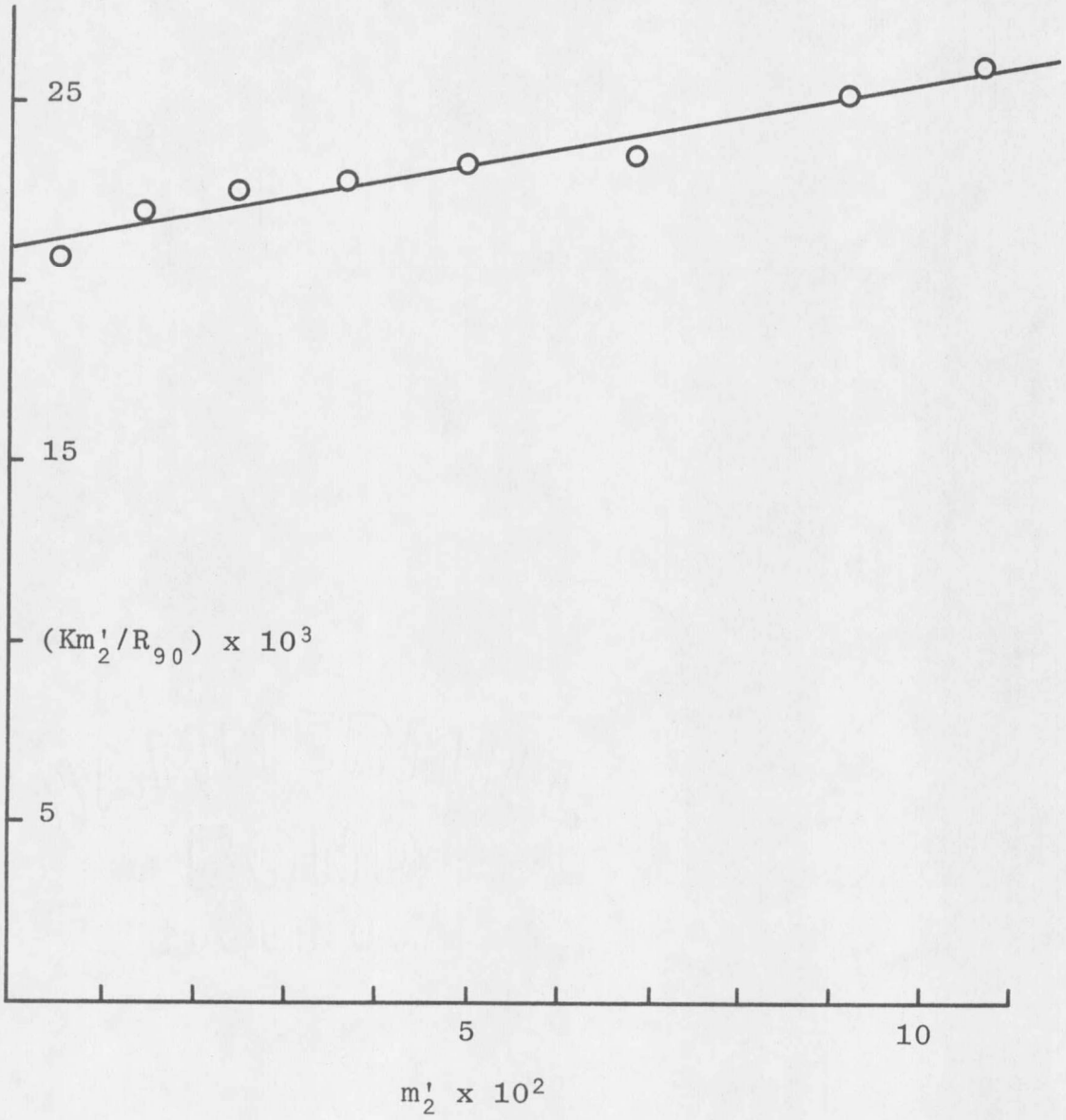

Best least squares straight line is included.

Fig. 18.--Scattering Data for DPB in 0.5 m NaBr, 25° C

Surfactant & Solvent	$K \times 10^5$	CMC $\times 10^3$	$n_2' \times 10^2$	Surfactant Molality $\times 10^2$	$R_{90} \times 10^5$
DPB in 0.5 m NaBr	4.39	11.06	5.11	0.56	0.02
				1.20	0.25
				1.68	1.22
				2.58	2.94
				3.58	4.86
				4.79	7.11
				6.14	9.52
				7.95	12.81
				10.33	16.07
				11.81	18.09
2M in 0.5 m NaBr	4.80	10.19	5.38	0.16	0.00
				0.58	0.02
				0.87	0.05
				1.24	0.43
				1.75	1.52
				2.46	2.93
				3.30	4.57
				4.20	6.34
				4.94	7.67
				5.52	8.68
				6.66	10.75
				7.39	11.93
3M in 0.5 m NaBr	4.80	8.87	5.34	0.45	0.02
				0.63	0.01
				1.08	0.41
				1.51	1.27
				2.18	2.58
				2.74	3.72
				3.45	5.11
				4.04	6.28
				4.73	7.64
				5.24	8.56
				6.08	10.12
				6.58	11.05
4M in 0.5 m NaBr	4.80	8.59	5.33	0.33	0.01
				0.62	0.02
				1.02	0.35
				1.23	0.79

4M (continued)				2.08	2.48
				2.68	3.67
				3.67	5.63
				3.90	5.98
				4.47	7.08
				5.30	8.75
				5.82	9.52
				7.36	12.35
2E in 0.5 m NaBr	5.31	7.60	5.63	0.51	0.00
				0.42	0.00
				0.31	0.01
				0.65	0.02
				1.11	0.72
				1.72	1.95
				2.38	3.18
				3.20	4.89
				3.62	5.64
				5.24	8.66
				6.02	10.06
				7.06	11.91
3E in 0.5 m NaBr	5.31	7.02	5.62	0.17	0.00
				0.38	0.01
				0.64	0.05
				1.30	1.38
				1.86	2.64
				2.70	4.43
				3.40	5.90
				4.70	8.71
				4.96	9.22
				5.42	10.14
4E in 0.5 m NaBr	5.30	6.90	5.76	0.21	0.02
				0.58	0.03
				0.68	0.15
				1.43	1.67
				2.09	3.06
				2.45	3.89
				3.10	5.27
				3.42	6.02
				4.20	7.65
				5.29	9.82
				6.09	11.55
				6.36	12.05

2MOL in 0.5 m NaBr	5.33	8.86	5.68	0.17	0.02
				0.29	0.02
				0.42	0.03
				0.68	0.04
				1.24	1.11
				2.02	3.49
				2.58	5.04
				3.20	6.90
				3.69	8.34
				4.28	10.02
				5.09	12.41
				6.25	15.75
3MOL in 0.5 m NaBr	5.33	10.59	5.48	0.14	0.00
				0.30	0.00
				0.50	0.02
				0.60	0.03
				1.16	0.32
				1.64	1.59
				2.45	3.59
				3.17	5.39
				3.84	6.94
				4.24	8.02
				4.93	9.82
				5.38	10.77
4MOL in 0.5 m NaBr	5.33	9.85	5.74	0.19	0.00
				0.34	0.01
				0.46	0.03
				0.60	0.03
				1.25	0.73
				1.80	2.20
				2.37	3.60
				3.02	5.22
				3.63	6.78
				4.42	8.72
				4.96	10.07
				5.49	11.29
4EOL in 0.5 m NaBr	6.25	10.24	6.10	0.15	0.02
				0.29	0.02
				0.32	0.03
				0.56	0.03
				1.05	0.11
				1.64	1.73

4EOL (continued)				2.22	3.32
				3.02	5.39
				3.54	6.52
				4.25	8.33
				4.70	9.63
				5.43	11.39
3POL in o.5 m NaBr	6.43	9.04	6.17	0.14	0.89
				0.29	0.89
				0.44	0.89
				0.82	0.93
				1.18	1.51
				1.74	2.77
				2.65	4.83
				3.26	6.18
				4.57	9.14
				4.78	9.71
				5.50	11.11
				6.33	12.94
4POL in 0.5 m NaBr	6.42	8.79	6.20	0.14	0.02
				0.28	0.03
				0.50	0.04
				0.81	0.07
				1.26	0.96
				1.69	1.96
				2.51	3.79
				3.24	5.64
				4.11	7.38
				5.44	10.20
				6.42	12.04
3MOM in 0.5 m NaBr	5.74	9.36	5.85	0.33	0.04
				0.50	0.05
				0.63	0.08
				1.32	0.91
				1.75	1.76
				2.41	3.13
				3.18	4.70
				4.06	6.45
				4.77	7.84
				5.47	9.23
				6.19	10.63

4MOM in 0.5 m NaBr	5.46	2.05	5.71	0.22	0.05
				0.30	0.20
				0.69	1.01
				1.23	2.20
3CN in 0.5 m NaBr	5.84	10.49	5.58	0.34	0.04
				0.64	0.06
				1.08	0.18
				1.55	1.58
				2.08	3.17
				2.65	5.08
4CN in 0.5 m NaBr (first run)	5.85	6.25	5.86	0.29	0.20
				0.47	0.40
				0.52	0.48
				3.29	13.52
				3.82	16.68
				4.48	20.99
4CN in 0.5 m NaBr (second run)	5.85	11.64	6.00	0.33	0.24
				0.73	0.52
				0.95	0.57
				1.21	0.57
				3.16	12.22
				3.72	15.56
				4.43	20.13
				5.16	24.87
				5.67	28.02
3BR in 0.5 m NaBr	6.13	8.01	6.04	0.23	0.02
				0.36	0.02
				0.49	0.04
				1.17	1.36
				1.55	2.68
				2.12	4.78
				2.77	7.39
				3.30	9.37
4MOL in 0.5 m NaCl	4.43	15.41	5.15	0.32	0.01
				0.63	0.04
				1.23	0.06
				1.81	0.52
				2.61	1.83
				3.15	2.73
				3.80	3.83

4MOL (continued)				4.50	5.02
				4.88	5.64
				5.58	6.85
				6.31	8.06
3BR in 0.5 m NaCl	5.27	14.56	5.62	0.22	0.02
				0.61	0.04
				0.92	0.07
				1.14	0.08
				1.59	0.35
				2.19	1.44
				2.78	2.56
				3.35	3.71
4CN in 0.5 m NaCl	5.07	35.98	5.48	0.06	0.08
				0.14	0.16
				0.19	0.30
				0.26	0.24
				3.91	0.54
				4.46	0.86
				5.33	1.30
				5.89	1.66
4TB in 0.5 m NaCl	5.34	7.90	5.66	0.36	0.04
				0.54	0.04
				1.31	0.97
				1.70	1.70
				2.46	2.98
				3.04	4.04
				3.58	4.89
				4.14	5.82
				4.91	7.18
3OH in 0.5 m NaCl	3.88	6.66	4.82	0.30	0.01
				0.71	0.12
				1.05	0.76
				1.38	1.31
				2.07	2.67
				2.70	3.78
				3.33	4.91
				3.99	6.07

3E in 0.5 m HBr	5.27	8.18	5.61	0.22	0.01
				0.29	0.03
				0.29	0.04
				1.39	1.35
				1.75	2.18
				2.35	3.51
				2.87	4.68
				3.27	5.58
3MOL in 0.5 m HBr	5.52	13.49	5.74	0.21	-0.01
				0.32	0.00
				0.35	0.02
				0.68	0.05
				1.69	0.97
				2.65	3.38
				3.51	5.72
				3.93	6.74
				4.46	7.98
				5.27	9.99
				6.11	12.15
3POL in 0.5 m HBr	7.19	12.25	6.54	0.14	0.01
				0.28	0.03
				0.45	0.04
				1.01	0.14
				1.73	1.37
				2.29	2.74
				3.04	4.67
				3.72	6.24
				4.06	7.13
3OH in 0.5 m HCl	4.24	9.76	5.05	0.26	0.01
				0.59	0.02
				0.87	0.04
				1.35	0.74
				2.00	1.97
				2.63	3.20
				3.12	4.10